IEEE Access
Multidisciplinary ⋮ Rapid Review ⋮ Open Access Journal

Received 24 February 2023, accepted 14 March 2023, date of publication 20 March 2023, date of current version 28 March 2023.

Digital Object Identifier 10.1109/ACCESS.2023.3259459

RESEARCH ARTICLE

Sizing of Microgrid System Including Multi-Functional Battery Storage and Considering Uncertainties

IBRAHIM M. IBRAHIM[1], ALMOATAZ Y. ABDELAZIZ[1], (Senior Member, IEEE), HASSAN HAES ALHELOU[2], (Senior Member, IEEE), AND WALID A. OMRAN[3]

[1]Faculty of Engineering, Ain Shams University, Cairo 11566, Egypt
[2]Department of Electrical and Computer Systems Engineering, Monash University, Clayton, VIC 3800, Australia
[3]Faculty of Engineering and Materials Science, German University in Cairo, Cairo 11835, Egypt

Corresponding author: Hassan Haes Alhelou (alhelou@ieee.org)

ABSTRACT Battery storage units (BSUs) are usually used to perform a single function in most planning studies related to microgrids (MGs). This paper presents an effective methodology to use the BSUs to perform multi-function including supply/demand matching and energy arbitrage. This is done according to a system policy containing all possible scenarios to fully utilize the BSUs to maximize the benefit. In the proposed work, the optimal sizing of the MG system under study containing wind turbines (WTs), photovoltaic system (PV), BSUs, and diesel units (DUs) is obtained. The main objectives of the proposed methodology are; 1) minimizing the total costs of the MG, 2) minimizing the harmful gas emissions, and 3) minimizing the accumulated power difference between the generation from renewable energy systems (RESs) and the demand. Due to the stochastic behavior of the output from the RESs, the uncertainties of wind speed, solar irradiance, and temperature are considered in the study. Two modes of operation of the MG (grid-connected and islanded) and the demand side management (DSM) are also considered. The problem is formulated as a constrained nonlinear optimization problem and is solved using two metaheuristic optimization algorithms, Moth-Flame Optimization (MFO) and Hybrid Firefly and Particle Swarm Optimization (HFPSO). Moreover, the uncertainties in the different parameters are considered by using the Latin Hypercube Sampling (LHS) method to generate samples of wind speed, solar irradiance, and temperature. To examine the proposed methodology, different case studies are presented and discussed. Moreover, the results of the used two algorithms, MFO and HFPSO, are compared to show their effectiveness in solving the proposed problem and assure the optimal solution. The optimization problem is implemented and solved using MATLAB software.

INDEX TERMS Energy arbitrage, microgrid, multi-functional battery, sizing, supply/demand matching, uncertainties.

I. INTRODUCTION

According to the definition of the MG by the U.S. energy department, the MG is an interconnection between a group of loads and distributed energy resources (DERs) within specific electrical boundaries. It behaves as a single controlled entity with respect to the utility grid (UG). It can operate in grid-connected mode or islanded mode [1]. The MG provides several benefits, including: 1) reducing power loss, 2) improving power quality, 3) enhancing reliability due to restoring loads or parts of the loads in the event of a fault in the UG, 4) increasing efficiency, and 5) helping in feeding far loads when the transmission and distribution infrastructures are not available. To improve the economic and technical aspects of the MGs, Energy storage systems (ESSs) are currently being widely utilized [2], [3], [4]. With respect to the technical aspects, the ESSs can be used to support voltage, regulate frequency, enhance stability, support

The associate editor coordinating the review of this manuscript and approving it for publication was Akin Tascikaraoglu.

reliability, enhance power quality, provide ride-through support, support the compensation of an unbalanced load, and perform peak shaving. With respect to the economic aspects, the ESSs can be used to gain a profit from energy arbitrage at which power is stored during low price hours to sell it to the UG during high price hours, reduce costs related to power quality or reliability problems, and gain profit from ancillary services such as voltage support and frequency regulation.

A. STUDY OBJECTIVE

The main objective of the proposed study is to present a new methodology to operate multi-functional BSUs that can enhance the performance of the MG system as follows:

- Function 1: supply/demand matching is to store the surplus power during the high-power time of the generation from the RESs and cover the deficit during the low-power time of the generation from the RESs.
- Function 2: energy arbitrage is to purchase the power from the UG during the off-peak time (low price) and sell it again during the on-peak time (high price) resulting in a profit.

This is done according to a proposed system policy to fully utilize the BSUs to maximize the benefit.

To obtain realistic results, the uncertainties of several parameters such as wind speed, solar irradiance, and temperature are considered in the study. In addition, the two modes of operation of the MG and the DSM are also considered.

B. RELATED LITERATURE SURVEY

Several studies addressed the use of the ESSs to improve the performance of the MGs. These studies can be classified into 1) grid-connected MG studies, 2) islanded MG studies, and 3) grid-connected and islanded MG studies. These studies are summarized in Table 1.

First, the grid-connected MG studies obtained the optimal sizing of the MG resources without considering the uncertainties of the RESs such as in [5], [6], and [7] or with taking it into consideration such as in [8], [9], and [10]. In [5], a study was proposed to obtain the size of the RESs in the first step and the size of the hybrid ESS containing BSU and super-capacitor (SC) in the second step. The objectives of this study were to minimize costs, improve reliability, and curtail emissions of the MG. The role of the hybrid ESS was to compensate for the difference between the generated and the demanded powers at any instant according to the frequency. In [6], the optimal sizing of the MG resources including RESs/BSUs was obtained. The objectives of this study were to minimize the bill of energy consumption via the use of the RESs and maximize the lifetime of the BSUs. The BSUs maintained the balance between the generation from the RESs and the demand. In [7], a comprehensive optimization model was proposed to obtain the sizing of the MG components including PV/BSU/grid converter. The study also contained a techno-economic model based on different variables. The objectives of this study were as follows: 1) maximizing the factors of the power and energy autonomy which measured the power and energy independence of the MG from the UG, respectively, 2) minimizing the capital costs of the MG, and 3) minimizing the simple payback period which measured the economic viability of the MG. The BSU was a primary source to ensure the match between the generation from the PV and the load. In [8], the optimal sizing and power dispatch of the MG resources including the RESs and the BSUs were obtained. The main objectives of this study were to minimize the total annual costs and maximize the profit of selling power to the UG. The uncertainties of the RESs and the load were considered in the study using suitable probability distribution functions (PDFs). The BSUs attenuated the fluctuations of the RESs. In [9], the optimal sizing of the MG resources including RESs/BSU was obtained in two phases. The optimal sizing of the RESs containing WT and PV was obtained in the first phase and the BSU in the second phase. This study aimed to minimize the total costs and maximize reliability. The uncertainty of the hourly wind speed was considered only from the RESs. The role of the BSU was to match the supply with the demand. In [10], a stochastic model was proposed to obtain the optimal size of the BSU. This model considered different economic and technical factors including BSU degradation, UG fluctuations, and reliability index. This study aimed to minimize the capital cost of the BSU, the operating cost of the MG, and the load curtailment cost. The uncertainties of the generation from the RESs and the dispatchable generators (DGs) were considered using the scenarios generation via Monte-Carlo Simulation (MCS) and the scenarios reduction via the fast-forward selection method. The BSU mitigated the fluctuations of the generated power from the RESs. The limitations of the aforementioned studies include the following: 1) the BSU performed only one function, although it could perform multi-function, 2) these studies considered only the grid-connected mode of the MG, 3) most of these studies did not consider the DSM, despite its benefits to the operation of the MG [11], 4) most of these studies did not consider the harmful gas emissions, despite their importance from the environmental aspect, 5) the uncertainties of the RESs were not considered in some of these studies.

Second, the islanded MG studies obtained the optimal sizing of the MG resources without considering the uncertainties of the RESs such as in [12], [13], and [14] or with taking it into consideration such as in [15] and [16]. In [12], the optimal design of the MG system containing RESs/BSUs/DUs was obtained. The objective of this study was to minimize the net present cost considering several constraints such as system reliability, customer satisfaction, and renewable energy use percentage. The BSUs covered the load in case of generation absence. In [13], the optimal sizing of the MG components containing RESs/BSUs/DUs was obtained. The objectives were to minimize the cost of energy (COE) and minimize the loss of power supply probability. The role of the BSUs was to do the supply/demand matching function. In [14], the optimal sizing of the MG components containing

TABLE 1. Related literature survey.

Ref.	Modes*	RESs	ESSs	ESSs functions	Uncertainties	DSM	Objectives	Optimization techniques
[2]	G & I	WT & PV	BSUs	- Load shifting or energy arbitrage in G - Unserved energy reduction in I	RESs & demand & electricity pricing	✗	- Minimize the investment cost of the BSUs and the operation cost of the MG in G - Minimize load curtailment cost in I	MILP
[5]	G	WTs & PV	BSU & SC	Supply-demand matching	✗	✗	- Minimize costs of the MG - Improve reliability of the MG - Curtail emissions of the MG	Iterative search algorithm
[6]	G	WT & PV	BSUs	Supply-demand matching	✗	✗	- Minimize the bill of energy consumption via the use of the RESs - Maximize the lifetime of the BSU	SQP
[7]	G	PV	BSU	Supply-demand matching	✗	✗	- Maximize the factors of the power and energy autonomy - Minimize the capital costs of the MG - Minimize the economic viability of the MG	PSO
[8]	G	WTs & PV	BSUs	Attenuation of the RESs fluctuations	RESs & demand	✓	- Minimize the total annual costs - Maximize the profit of selling power to the UG	MILP
[9]	G	WT & PV	BSU	Supply-demand matching	Wind speed	✗	- Minimize the total costs - Maximize the reliability	Two constrained based iterative search algorithms
[10]	G	WT & PV	BSU	Mitigation of the RESs fluctuations	RESs & DGs	✗	- Minimize the capital cost of the BSU - Minimize the operating cost of the MG - Minimize the load curtailment cost	MIQP
[12]	I	WTs & PV	BSUs	Supply-demand matching	✗	✗	Minimize the net present cost	EO, AEFA, HHO, STOA, and GWO
[13]	I	WTs & PV	BSUs	Supply-demand matching	✗	✗	- Minimize the cost of energy - Minimize the loss of power supply probability	hHHO-AOA
[14]	I	WTs & PV	BSUs	Keeping a constant power flow to the load	✗	✗	- Minimize the cost of energy - Maximize the reliability	WOA, MFO, WCA, and PSOGSA
[15]	I	PV	BSUs & HSUs	Supply-demand matching	PV & demand	✗	Minimize the total costs of the system	GA and MILP
[16]	I	WT & PV	BSU	storing the excess energy	RESs & demand	✗	Minimize the total costs (planning and operational).	SQP & PSO

* MG modes are: grid-connected (G) and islanded (I)

RESs/BSUs/DU was obtained to minimize the COE and maximize the reliability. The role of the BSUs was to keep a constant power flow to the load. In [15], the optimal sizing of the MG resources containing PV, hydrogen storage units (HSUs), and BSUs was obtained to minimize the total costs of the system. Then, a unit commitment problem was proposed to obtain the optimal plan of operation. The BSUs and HSUs were auxiliary storages to ensure the balance between the generation and the demand. The optimal sizing of the MG resources containing RESs/ESS/DU/biogas generator was obtained in [16] to minimize the total costs (planning and operational). The ESS stored the excess energy after demand satisfaction. Similarly, the aforementioned islanded MG studies contained the same limitations as the grid-connected studies including considering one function of the BSU, considering one mode of operation of the MG, the absence of DSM, the absence of the environmental aspect, and the application of the deterministic approach in several studies.

Finally, the grid-connected and islanded MG modes were considered in some studies such as in [2]. In this study, an expansion planning model was proposed to obtain the optimal size, technology, number, and maximum depth of discharge of the BSUs. The objective of this study was to minimize the investment cost of the BSUs and the operation cost of the MG (in the grid-connected mode only) or load curtailment cost (in the islanded mode only). The uncertainties of RESs, demand, and electricity pricing were considered depending on the forecasted data. The BSUs performed either load shifting or energy arbitrage in the grid-connected mode and reduced the unserved energy in the islanded mode.

Compared to the proposed methodology, the limitations of the study in [2] are as follows: 1) the study did not aim to size the MG generation units as well as the BSUs. It rather aimed to upgrade an existing MG with BSUs, 2) the study did not clarify if the BSUs could perform both functions at the same time, 3) the study did not consider the harmful gas emissions, despite their importance from the environmental aspect, 4) the study did not clarify how the DSM was used, despite mentioning that one of the objectives was to perform load shifting, 5) the study aimed to minimize the cost without replacing the

BSUs. However, this did not allow the utilization of the full capabilities of the BSUs, especially because no system policy or Energy Management System (EMS) was used, 6) The uncertainties were considered using the forecasting errors which is not an accurate representation of the data due to the lack of different scenarios, and 7) the performance of the MG was not clearly presented during the worst-case scenario, in which the generation is lower than the demand, the BSUs are fully discharged, and the power deficit is higher than the grid limit.

C. OPTIMIZATION TECHNIQUES

The previously mentioned studies used several optimization techniques which can be classified into three main categories as follows: 1) mathematical optimization techniques, 2) metaheuristic optimization algorithms, and 3) hybrid metaheuristic optimization techniques.

First, mathematical optimization techniques such as Mixed Integer Linear Programming (MILP), Sequential Quadratic Programming (SQP), Mixed Integer Quadratic Programming (MIQP), and iterative search algorithms have good convergence characteristics. On the other hand, its obtained optimal solution, especially in the complex constrained non-linear optimization problems, may be a local optimal solution and not a global one. This is due to the dependence of these techniques on the initial value and gradient information [17], [18].

Second, metaheuristic optimization algorithms are divided into four types as follows [19], [20], [21]:

i) swarm intelligence-based algorithms that depend on the social behavior of insects, birds, animals, fishes, etc. Examples of this category are; Moth-Flame Optimization (MFO), Particle Swarm Optimization (PSO), Firefly Algorithm (FA), Grey Wolf Optimization (GWO), Harris Hawks Optimizer (HHO), Sooty Tern Optimization Algorithm (STOA), Whale Optimization Algorithm (WOA), and Water Cycle Algorithm (WCA).

ii) physics-based algorithms that depend on the physical rules in the universe (related to gravity, inertia, mass, volume, etc.) such as Equilibrium Optimizer (EO), Artificial Electric Field Algorithm (AEFA), Arithmetic Optimization Algorithm (AOA), and Gravitational Search Algorithm (GSA).

iii) Evolutionary algorithms that depend on natural evolution like genetic recombination, mutation, and natural selection. Examples of this category are; Genetic Algorithm (GA) and Differential evolution (DE).

iv) human-based algorithms that depend on human behavior such as Teaching Learning-Based Optimization (TLBO) and Tabu Search (TS).

Compared to mathematical optimization techniques, metaheuristic optimization algorithms can solve complex optimization problems effectively and obtain the global optimal solution in less time [22], [23], [24]. These techniques are suitable to handle MG optimization problems due to their flexibility, robustness, efficiency, accuracy, and short convergence time [22]. Due to the previous advantages, the metaheuristic optimization algorithms are more suitable for solving non-convex optimization problems which have global and local solutions [18], [25], [26], [27]. Moreover, it can solve the convex optimization problem effectively. However, these techniques need tuning of specific parameters to ensure convergence to the global optimal solution.

Finally, hybrid optimization techniques depend on the combination of two or more different techniques to overcome their shortcomings and merge their strengths. Examples of this category are; hybrid Harris Hawks Optimizer and Arithmetic Optimization Algorithm (hHHO-AOA) and Hybrid Particle Swarm-Gravitational Search Algorithm (PSOGSA).

In the proposed work, two metaheuristic optimization algorithms are chosen to obtain the global optimal solution of the constrained non-linear optimization problem under study. These algorithms are as follows:

- Moth-Flame Optimization (MFO) algorithm which is considered one of the swarm intelligence-based algorithms.
- Hybrid Firefly and Particle Swarm Optimization (HFPSO) algorithm which is considered one of the hybrid optimization techniques.

A comparison is done between them to check the aforementioned advantages of the metaheuristic optimization algorithms either individual or hybrid and assure the optimal solution of the proposed optimization problem.

D. CONTRIBUTIONS AND PAPER ORGANIZATION

Compared to the previously mentioned studies, the main contributions of this work include the following:

- The BSUs are used to perform multi-function including supply/demand matching and energy arbitrage to enhance the performance of the MG system under study,
- Environmental aspect is considered,
- Two operation modes of the MG, grid-connected and islanded, are considered,
- The DSM is considered, and
- The uncertainties of the RESs including wind speed, solar irradiance, and temperature are considered.

The organization of this paper is as follows: the system under study and the proposed system policy of the MG are introduced in Section II. The modeling of uncertainties is presented in Section III. In Section IV, the proposed optimization problem is formulated. The optimization algorithms that are used to solve the formulated sizing problem are discussed in Section V. In Section VI, the case studies and the obtained results are presented and discussed. Finally, the conclusions are summarized in Section VII and the future work is mentioned in Section VIII.

II. MG OPERATION POLICY

This section includes the MG system under study and the MG operation policy.

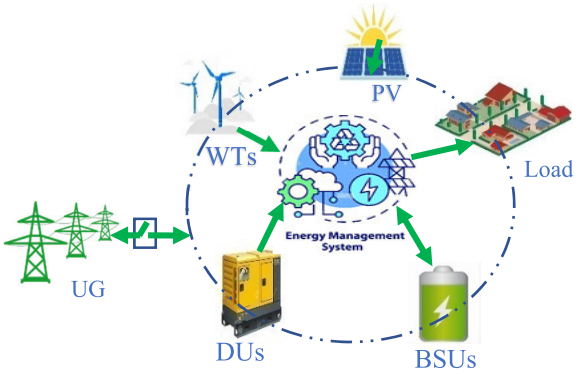

FIGURE 1. The MG system under study.

A. THE MG SYSTEM UNDER STUDY

Fig. 1 shows the architecture of the MG under study. It includes the following: 1) RESs including WTs and PV, 2) BSUs, 3) DUs, 4) Load demand, and 5) EMS which ensures the execution of the proposed system policy to fully utilize the BSUs capabilities. The connection between the MG and the UG is assumed to be through a single point of interconnection.

The BSUs are considered to perform two functions to enhance the performance of the MG as follows:

- Function 1: supply/demand matching is to store the surplus power during the high-power time of the generation from the RESs and cover the deficit during the low-power time of the generation from the RESs.
- Function 2: energy arbitrage is to purchase the power from the UG during the off-peak time (low price) and sell it again during the on-peak time (high price) resulting in a profit.

The DUs are used to cover the deficit between the generation from the RESs and the demand in case of the unavailability of the BSUs and the UG.

The DSM is used in this study to control the demand of the MG in different cases by dividing the loads into three different categories as follows: (1) Essential Demand (ED) that is completely supplied at its desired time, (2) Partially Shiftable/Curtailable Demand (PSCD) at which the unsupplied part of the demand can be shifted to another time within the same day when there is surplus power from the RESs and the remaining part may be curtailed. In this case, the customers receive money credits for both the shifted and curtailed parts of the demand. Finally, (3) Partially Curtailable Demand (PCD) at which the unsupplied part of the demand can be totally curtailed in case of generation deficit; hence, the customers receive money credit for the curtailed demand. The demand of the second and third categories that must be supplied after using the DSM equals 60% of the demand before using the DSM. In the proposed methodology, the percentage of the fixed loads is assumed to be 60% while the shiftable/curtailable loads are 40%. These percentages are determined depending on the types of loads in the demand of the MG system and the request of the project owner [28].

B. THE SYSTEM POLICY OF THE MG

To ensure the proper operation of the MG and the proper use of the BSUs, several expert system rules should be considered to develop the system policy. In this work, the system policy is divided into six cases to cover all possible scenarios between the generation from the RESs, the demand, the time of use, and the connection status between the MG and the UG as shown in Fig 2. These cases can be summarized as follows:

1) GENERATION ≥ DEMAND, OFF-PEAK TIME, GRID-CONNECTED MODE (G≥D, FP, GC)

- Firstly, the demand is satisfied by the RESs. This demand may be the first type (ED) or the second type (PSCD) according to the generation from the RESs at this moment.
- Secondly, the BSUs are charged from the surplus power of the RESs (Function 1).
- Thirdly, if this surplus power cannot fully charge the BSUs, additional power is purchased from the UG until it is fully charged (Function 2).
- Finally, any additional excess power from the RESs after fully charging the BSUs is sold to the UG up to the grid limit otherwise, the RESs power is curtailed.

2) GENERATION ≥ DEMAND, ON-PEAK TIME, GRID-CONNECTED MODE (G≥D, NP, GC)

- Firstly, the demand is satisfied by the RESs. This demand may be the first type (ED) or the second type (PSCD) according to the generation from the RESs at this moment.
- Secondly, the surplus power from the RESs is sold to the UG up to the grid limit.
- Thirdly, the excess power above the grid limit is used to charge the BSUs (Function 1). If the BSUs are fully charged, then the remaining power from the RESs is curtailed.
- Finally, the BSUs are discharged to sell the power to the UG (Function 2) up to the grid limits.

3) GENERATION < DEMAND, OFF-PEAK TIME, GRID-CONNECTED MODE (G<D, FP, GC)

- Firstly, a part of the demand is satisfied by the RESs. This demand may be one of two types, either the PSCD or the PCD, according to the availability of the RES.
- Secondly, the power deficit between the generation from the RESs and the demand is satisfied by buying the power from the UG.
- Thirdly, if the power deficit is higher than the grid limit, the remaining power will be taken from the BSUs (Function 1). If the BSUs are fully discharged, the remaining power will be taken from the DUs.
- Finally, the power is purchased from the UG to charge the BSUs to be fully charged if the power deficit is satisfied (Function 2).

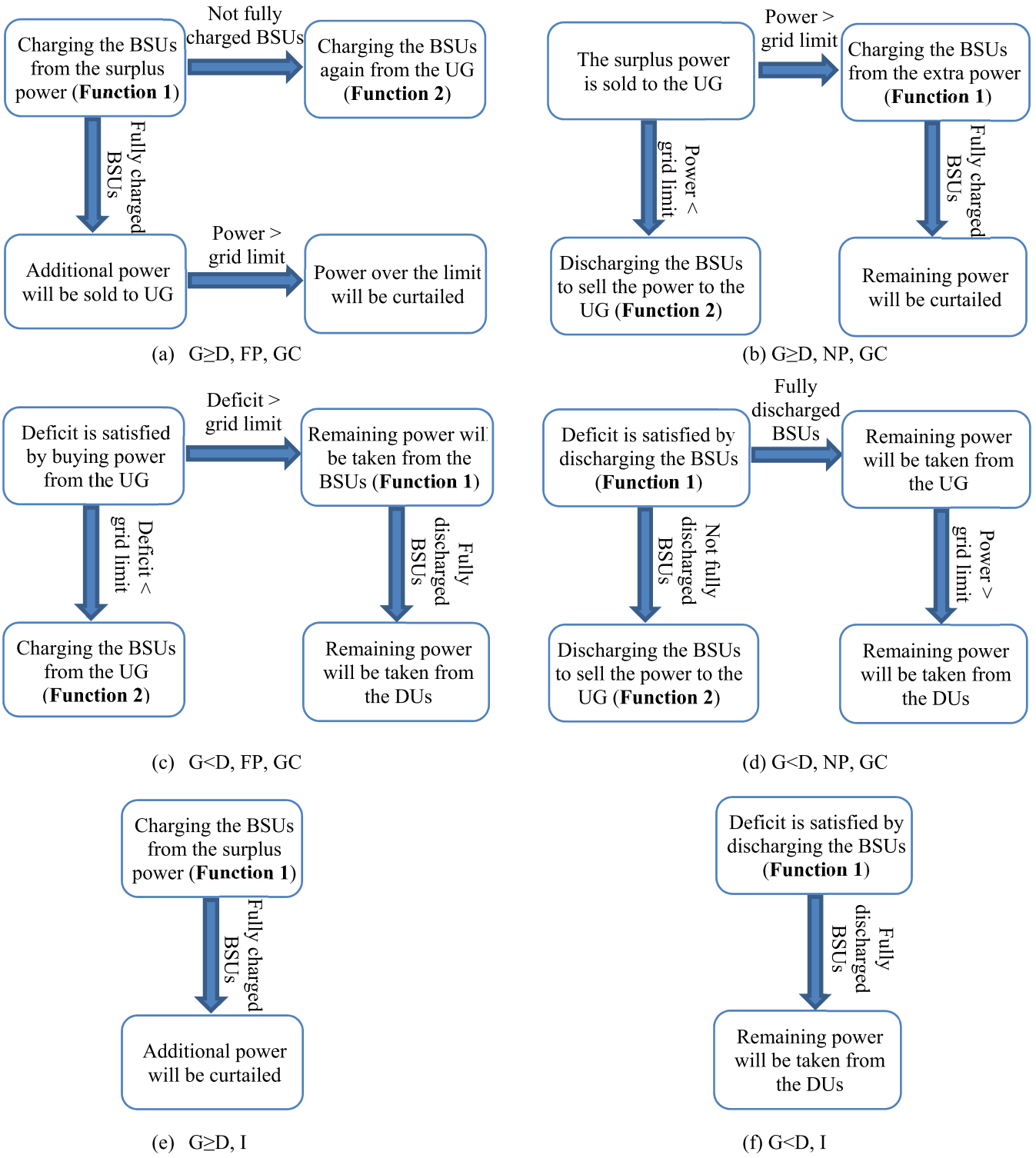

FIGURE 2. MG system policy cases (six cases).

4) GENERATION < DEMAND, ON-PEAK TIME, GRID-CONNECTED MODE (G<D, NP, GC)

- Firstly, a part of the demand is satisfied by the RESs. This demand may be one of two types, either the PSCD or the PCD, according to the availability of the RES.
- Secondly, the power deficit is satisfied by discharging the BSUs (Function 1).
- Thirdly, if the BSUs are fully discharged, the required power is purchased from the UG. If the required power is higher than the grid limit, the power is taken from the DUs.

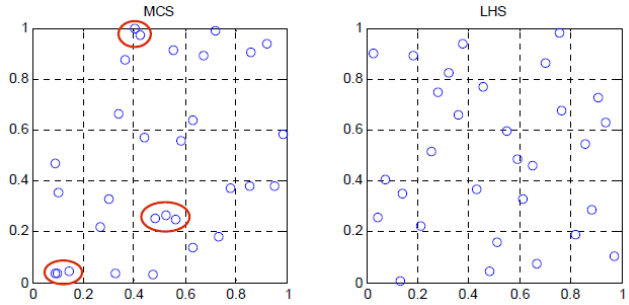

FIGURE 3. Comparison between MCS and LHS methods in sampling.

- Finally, if the deficit is satisfied and the BSUs are not fully discharged, the BSUs are discharged to sell the power to the UG up to the grid limits (Function 2).

5) GENERATION ≥ DEMAND, ISLANDED MODE (G≥D, I)

- Firstly, the demand is satisfied by the RESs. This demand may be the ED or the PSCD according to the generation from the RESs at this moment.
- Secondly, the BSUs are charged from the surplus power of the RESs (Function 1).
- Finally, if the BSUs are fully charged, the remaining power from the RESs is curtailed.

6) GENERATION < DEMAND, ISLANDED MODE (G<D, I)

- Firstly, a part of the demand is satisfied by the RESs. This demand may be one of two types, either the PSCD or the PCD, according to the availability of the RES.
- Secondly, the power deficit is satisfied by discharging the BSUs (Function 1).
- Finally, if the BSUs are fully discharged and the power deficit is not satisfied, the required power will be taken from the DUs.

III. MODELING OF UNCERTAINTIES

A. LATIN HYPERCUBE SAMPLING (LHS) METHOD

The LHS method divides the sample space into small regions (hypercubes) with equal probability and then generates the samples within these regions. The generated samples fill the regions effectively without clustering the generated samples together which may occur in the Monte Carlo Simulation (MCS) method.

The LHS method is used in the proposed work due to two main advantages compared to the MCS [29], [30], [31], [32]:

- Higher efficiency in sampling as shown in Fig. 3. As a result, the original probability distribution of the uncertain parameters is fully maintained in the produced samples, and
- Lower number of simulations and computations.

The steps of the LHS method can be summarized as follows [32]:

1) Dividing the sampling space of the uncertain parameter into n intervals with equal probability.
2) Obtaining the probability of randomly selected number (s_{ii}) from the interval [ii-1/n, ii/n]. The number is selected using the following equation:

$$s_{ii} = \frac{num}{n} + \frac{ii-1}{n}, ii = 1, 2, .., n \tag{1}$$

where n is the number of intervals in the sampling space of the LHS method and num is a random number in the range [0,1].
3) Transforming the obtained probabilities in step (2) into the corresponding samples values using the inverse transformation of the probability density function using the following equation

$$x_{ii} = F^{-1}(s_{ii}) \tag{2}$$

where x_{ii} is the corresponding sample value of the randomly selected number s_{ii} and F^{-1} is the inverse of the probability distribution function.

B. MODELING UNCERTAINTIES IN WIND SPEED, SOLAR IRRADIANCE, AND TEMPERATURE

There are several steps to consider the uncertainties of the wind speed, solar irradiance, and temperature in the proposed work as follows:

1) The historical data (10 years) of the hourly wind speed, solar irradiance, and temperature are obtained [33].
2) The obtained historical data are classified into twelve months and then a suitable distribution fitting is obtained for each hour in each month. The Weibull distribution function is used to fit the wind speed data and the Normal (Gaussian) distribution function is used to fit the solar irradiance and temperature data [8], [34], [35], [36]. The probability distribution function or probability density function (PDF) of the Weibull distribution function is calculated using the following equation:

$$f(v) = \frac{k}{c}\left(\frac{v}{c}\right)^{k-1} exp\left(-\left(\frac{v}{c}\right)^{k}\right) \tag{3}$$

where k and c are the shape and scale parameters of the Weibull function (positive scalar values), respectively. In Equation (3), the hourly wind speed data are converted to be at the hub height of the turbine using the following power-law equation [37]:

$$\frac{v}{v_o} = \left(\frac{h}{h_o}\right)^{0.143} \tag{4}$$

where v and v_o are wind speeds (m/s) at height h and h_o, respectively. h and h_o are the hub height of the WT ($h = 50$ m) and the height of the wind speed data ($h_o = 10$ m), respectively.
The PDF of the Normal distribution function is calculated using the following equation:

$$f(x) = \frac{1}{\sigma\sqrt{2\pi}} exp\left(\frac{-(x-\mu)^2}{2\sigma^2}\right) x \in \mathbb{R} \tag{5}$$

TABLE 2. Weibull and normal distribution fittings at 6 am.

Data	Wind speed	Solar irradiance	Temperature
PDF	Weibull	Normal	Normal
Parameter 1	$C = 5.2833$	$\sigma = 119.5024$	$\sigma = 10.4911$
Parameter 2	$K = 2.3076$	$\mu = 26.0039$	$\mu = 2.008$

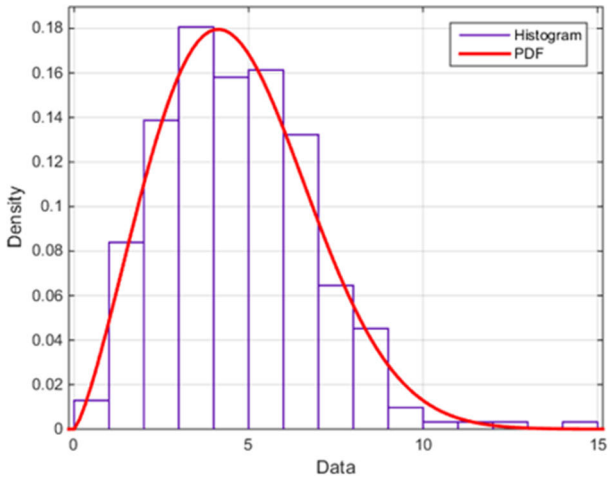

FIGURE 4. Histogram and PDF of the January wind speed data at 6 am.

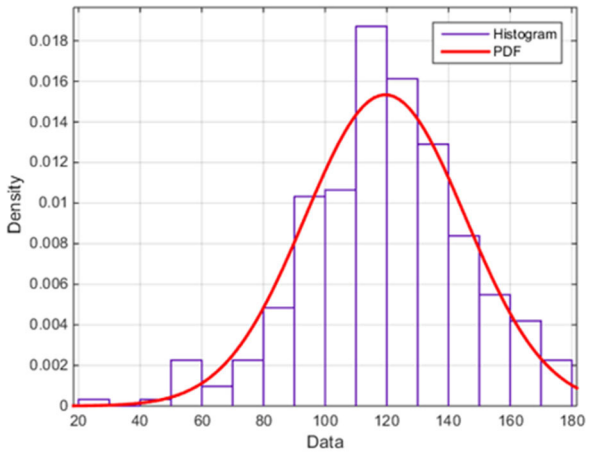

FIGURE 5. Histogram and PDF of the January solar irradiance data at 6 am.

where μ and σ are the mean ($-\infty < \mu < \infty$) and the standard deviation ($\sigma \geq 0$) of the Normal distribution, respectively.

As an example, Table 2 shows the obtained parameters from the Weibull and Normal distribution fittings for the wind speed, solar irradiance, and temperature at hour 6 am in January month, respectively. Fig. 4, Fig. 5, and Fig. 6 show the histogram and the PDF of the January wind speed, solar irradiance, and temperature at 6 am, respectively.

3) Using the LHS method, 100 scenarios of each hour in each month are generated for the wind speed, solar irradiance, and temperature. This is done by using the parameters obtained in Step (2) to obtain a distribution with the same parameters for each hour and then generate the samples which represent this distribution for each hour in each month. Finally, 100 scenarios of one year for the hourly wind speed, solar irradiance, and temperature are obtained to be used in the stochastic optimization problem.

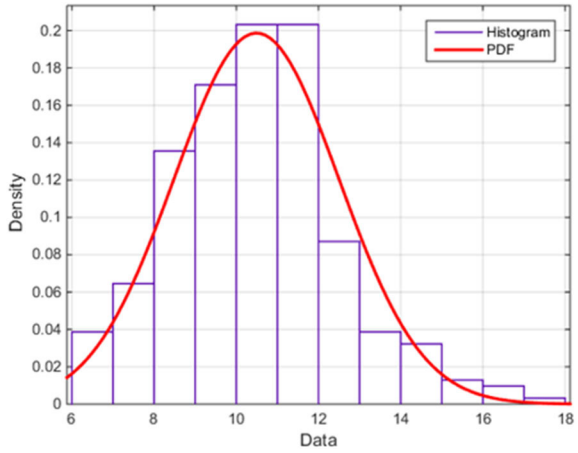

FIGURE 6. Histogram and PDF of the January temperature data at 6 am.

IV. OPTIMIZATION PROBLEM FORMULATION

The objective of the formulated problem is to find the sizes of the RESs, BSUs, and the DUs to achieve the main objectives of the proposed study as follows:

- First objective:
  This objective is achieved by minimizing the total costs of the MG system including initial costs, operation and maintenance costs, costs of purchasing/selling energy from/to the UG, penalty costs due to emissions from the DUs, curtailment costs, and salvage costs.
- Second objective:
  This objective is achieved by minimizing the costs related to the emissions of the harmful gases produced by the DUs. These harmful gases include CO_2, N_2O, and CH_4 [38].
- Third objective:
  This objective is achieved by minimizing the accumulated power difference between the generation from the RESs and the demand within the MG system.

The proposed optimization problem is a nonlinear multi-objective problem and is converted into a single-objective problem using the weighted sum method. The objective function of the proposed optimization problem can be described using (6)-(20) as follows:

$$Minimize\ Obj = W_1 \frac{C_{total}}{C_{totalmax}} + W_2 \frac{\Delta \hat{P}}{\Delta \hat{P}_{max}} \tag{6}$$

$$C_{total} = C_{in} + PWF_1(C_{op} + C_{gr} + C_{em} + C_{cu}) - PWF_2(C_{sa}) \tag{7}$$

$$C_{in} = C_{i,WT} N_{WT} P_{WT}^{cap} + C_{i,PV} N_{PV} P_{PV}^{cap}$$

$$+ C_E E_B^{cap} + C_P P_B^{cap} + C_{diesel} P_{diesel}^{cap} \quad (8)$$

$$C_{op} = C_{O,WT} N_{WT} P_{WT}^{cap} + C_{O,PV} N_{PV} P_{PV}^{cap} + C_O P_B^{cap} + C_{O,diesel} \quad (9)$$

$$C_{o,diesel} = a_f \sum_{t=1}^{T} P_{diesel}^2(t) + b_f \sum_{t=1}^{T} P_{diesel}(t) + c_f T_{diesel} \quad (10)$$

$$C_{gr} = \sum_{t=1}^{T} C_b(t) P_{U-M}(t) - \sum_{t=1}^{T} C_s(t) P_{M-U}(t) \quad (11)$$

$$C_{em} = \left(a_e \sum_{t=1}^{T} P_{diesel}^2(t) + b_e \sum_{t=1}^{T} P_{diesel}(t) + T_{diesel} \right) \left(\alpha_{CO_2} + \alpha_{N_2O} + \alpha_{CH_4} \right) C_{em-coeff} \quad (12)$$

$$C_{cu} = C_{cu\_G} + C_{cu\_D} \quad (13)$$

$$C_{cu\_G} = C_{dump} E_{dump} \quad (14)$$

$$C_{cu\_D} = C_{sh} \sum_{t=1}^{T} P_{sh}(t) + C_{nonsh} \sum_{t=1}^{T} P_{nonsh}(t) \quad (15)$$

$$C_{sa} = 0.1 C_{in} \quad (16)$$

$$PWF_1 = \frac{(1+d)^l - 1}{d(1+d)^l} \quad (17)$$

$$PWF_2 = \frac{1}{(1+d)^l} \quad (18)$$

$$\Delta \hat{P} = \sum_{t=1}^{t=T} |\Delta p(t)| \quad (19)$$

$$\Delta p(t) = \left(N_{pv} P_{pv}(t) + N_{wt} P_{wt}(t) \right) - P_{d-DSM}(t) \quad (20)$$

where W_1 and W_2 are the weights of the objectives in the objective function, $C_{total\,max}$ is the maximum value of the total costs of the MG ($), $\Delta \hat{P}_{max}$ is the maximum value of the accumulated power difference between the generation from the RESs and the demand after the DSM (kW), C_{total} is the total costs of the MG ($), $\Delta \hat{P}$ is the accumulated power difference between the generation from the RESs and the demand after the DSM (kW), $C_{in}, C_{op}, C_{gr}, C_{em}, C_{cu}$, and C_{sa} are the initial costs, operation and maintenance costs, purchasing/selling energy from/to the UG costs, penalty costs due to produced emissions from the DUs, curtailment costs, and salvage costs ($), respectively, PWF_1 and PWF_2 are present worth factors to convert the costs from annual value into present value and from future value into present value, respectively, $C_{i,WT}, C_{i,PV}, C_{O,WT}$, and $C_{O,PV}$ are the initial cost and the operation and maintenance cost of the WTs and the PV ($/kW), respectively, C_E, C_P, and C_O are the initial cost per unit energy ($/kWh), initial cost per unit power ($/kW), and operation and maintenance cost ($/kW) of the BSUs, respectively, C_{diesel} and $C_{O,diesel}$ are the initial cost ($/kW), and operation and maintenance cost ($) of the DUs, respectively, $C_b(t)$ and $C_s(t)$ are the instantaneous price of buying/selling energy from/to the UG ($/kWh), respectively, $C_{em-coeff}$ is the penalty cost coefficient of the emissions produced from the DUs ($/kg), C_{cu_G} and C_{cu_D} are the total costs of generation curtailment and demand curtailment ($), respectively, C_{dump} is the cost of dumped energy from the generation ($/kWh), C_{sh} and C_{nonsh} are the penalty costs of the demand to be shifted to another time (shiftable) and the demand to be curtailed (non-shiftable) ($/kWh), respectively, N_{WT} and N_{PV} are the numbers of the WTs and PV, respectively, $P_{WT}^{cap}, P_{PV}^{cap}, P_B^{cap}$, and P_{diesel}^{cap} are the power ratings of WT, PV, BSUs, and DUs (kW), respectively, E_B^{cap} is the energy rating of BSUs, a_f, b_f, *and* c_f are the coefficients of the fuel cost of the DUs ($/kW^{2}h, $/kWh, and $/h), respectively, a_e, b_e, and c_e are the coefficients of emissions of the DUs (L/kW^{2}h, L/kWh, and L/h), respectively, $\alpha_{CO_2}, \alpha_{N_2O}$, and α_{CH_4} are the coefficients of the gases CO_2, N_2O, and CH_4 produced from the DUs (kg/L), respectively, $P_{U-M}(t)$ and $P_{M-U}(t)$ are the instantaneous purchased power from the UG to the MG and the sold power from the MG to the UG, respectively (kW), $P_{diesel}(t)$, $P_{sh}(t)$, $P_{nonsh}(t)$, $P_{PV}(t)$, $P_{WT}(t)$, and $P_{d-DSM}(t)$ are the instantaneous DUs output power, shiftable demand power, non-shiftable demand power, PV output power, WTs output power, and demand power after applying the DSM (kW), respectively, E_{dump} is the total dumped energy from the RESs (kWh), T_{diesel} is the working hours of the DUs, $\Delta p(t)$ is the instantaneous power difference between the generation from the RESs and the demand after the DSM (kW), d is the average annual discount rate, l is the number of years per the study period (years), T is the total hours per the study period, and t is the time index.

The objective function (6) includes two terms. The first term represents the total costs of the MG which are calculated by (7). The second term represents the accumulated power difference between the generation from the RESs and the demand after applying the DSM which is calculated by (19). The total costs of the MG include the initial costs as in (8), operation and maintenance costs as in (9), the costs of purchasing/selling energy from/to the UG as in (11), the penalty costs due to produced emissions as in (12), curtailment costs as in (13), and salvage costs as in (16).

The curtailment costs are divided into the costs of generation curtailment and demand curtailment which are calculated by (14) and (15). The present worth factors in (17) and (18) are used to convert the annual value and the future value of the annual and the future costs in (7) into present value, respectively. Equations (19) and (20) calculate the accumulated power difference between the generation from the RES and the demand after applying the DSM.

The optimization problem is subjected to several technical constraints as follows:

The power balance of the MG system:

$$N_{PV} P_{PV}(t) + N_{WT} P_{WT}(t) \pm P_B(t) + P_{diesel}(t) + P_{U-M}(t) - P_{M-U}(t) - P_{dump}(t) - P_{d-DSM}(t) - P_{losses}(t) = 0, \quad \forall t \quad (21)$$

The constraints related to the BSUs:

$$E_B(t+\Delta t) = E_B(t) + \Delta t P_B(t)\,\eta_{ch} \quad \forall t \tag{22}$$

$$E_B(t+\Delta t) = E_B(t) - \Delta t \frac{P_B(t)}{\eta_{disch}} \quad \forall t \tag{23}$$

$$0 \le P_B(t) \le P_B^{cap} \quad \forall t \tag{24}$$

$$SoC_{min} E_B^{cap} \le E_B(t) \le SoC_{max} E_B^{cap} \quad \forall t \tag{25}$$

$$E_{B,min}^{cap} \le E_B^{cap} \le E_{B,max}^{cap} \tag{26}$$

$$E_B(1) = E_B^{cap} \tag{27}$$

The constraint related to the DUs:

$$0 \le P_{diesel}(t) \le P_{diesel}^{cap} \quad \forall t \tag{28}$$

The constraints related to the RESs:

$$P_{WT}(t) = \begin{cases} 0; & v_{co} \le v_w(t) < v_{ci} \\ P_{WT}^{cap} \times \dfrac{v_w(t) - v_{ci}}{v_r - v_{ci}}; & v_{ci} \le v_w(t) < v_r \\ P_{WT}^{cap}; & v_r \le v_w(t) < v_{co} \end{cases} \tag{29}$$

$$P_{PV}(t) = f_{PV} P_{PV}^{cap} \frac{G(t)}{G_{STC}} [1 + \alpha_T (T(t) - T_{STC})] \tag{30}$$

$$N_{WT,min} \le N_{WT} \le N_{WT,max} \tag{31}$$

$$N_{PV,min} \le N_{PV} \le N_{PV,max} \tag{32}$$

The constraint related to the MG-UG:

$$-P_{grid\,max}\varepsilon \le P_{U-M}(t) \le P_{grid\,max}\varepsilon \tag{33}$$

$$-P_{grid\,max}\varepsilon \le P_{M-U}(t) \le P_{grid\,max}\varepsilon \tag{34}$$

$$\varepsilon = \begin{cases} 1 & \text{Grid} - \text{connected} \\ 0 & \text{Islanded} \end{cases} \tag{35}$$

where $P_B(t)$, $P_{dump}(t)$, and $P_{losses}(t)$ are the instantaneous BSUs power, curtailed power from the RESs, and power losses (5% of the demand power) (kW), respectively, $E_B(t)$ is the instantaneous energy of the BSUs (kWh), η_{ch} and η_{disch} are the charging and discharging efficiency of the BSUs, respectively, Δt is the data time step (1 hour), SoC_{min} and SoC_{max} are the minimum and maximum state of charge of the BSUs, respectively, $E_{B,min}^{cap}$ and $E_{B,max}^{cap}$ are the lower and upper limits of the energy rating of the BSUs, respectively, $v_w(t)$ is the instantaneous wind speed (m/s), v_{ci}, v_{co}, *and* v_r are the cut-in, cut-out, and rated wind speed (m/s), respectively, f_{PV} is the derating factor of the PV, $G(t)$ and $T(t)$ are the instantaneous solar irradiance (W/m^2) and temperature (°C), respectively, G_{STC} *and* T_{STC} are solar irradiance and temperature at the standard conditions, respectively, α_T is the temperature coefficient, $N_{PV,min}$,$N_{WT,min}$,$N_{PV,max}$, *and* $N_{WT,max}$ are the lower and the upper limits of the PV and WTs number, respectively, $P_{grid\,max}$ is the maximum allowable limit of the power transfer between the MG and the UG (kW), and ε is the status of the connection between the MG and the UG.

First, Constraint (21) ensures that the power balance of the MG must be satisfied at each time interval.

Second, the constraints related to the BSUs include (22) and (23) which describe the charging and the discharging of the BSUs, (24)-(26) which ensure that the instantaneous power, the instantaneous energy, and the energy capacity of the BSUs must be within the lower and the upper limits, and (27) assumes that the BSUs are fully charged at the start of the study period.

Third, Constraint (28) ensures that the instantaneous power of the DUs must be within the lower and the upper limits.

Fourth, the constraints related to the RESs include (29) and (30) which calculate the instantaneous power of the RES, and (31) and (32) which ensure that the numbers of the WTs and PV must be within the lower and the upper limits.

Fifth, the constraints related to the power transfer between the MG and the UG include (33)-(35) which ensure that the purchasing/selling of the energy from/to the UG must be within the maximum allowable limits. Equation (35) shows that the MG is either grid-connected or islanded. The islanding of the MG is classified into intentional islanding and unintentional islanding according to IEEE standard 1547-2018 [39], [40]. The islanding hours are assumed to be 10% of the total hours.

V. METAHEURISTIC OPTIMIZATION ALGORITHMS

The formulated optimization problem is solved using two metaheuristic optimization algorithms: the moth-flame optimization (MFO) algorithm and the hybrid firefly and particle swarm optimization (HFPSO) algorithm.

A. MOTH-FLAME OPTIMIZATION (MFO) ALGORITHM

Several studies used the MFO algorithm in solving the optimization problems related to the power systems, especially the MG, and mentioned that the MFO obtained the best solution compared to other algorithms such as in [41], [42], and [43]. The MFO algorithm [44], [45] is a metaheuristic optimization algorithm that depends on the behavior of the moths' insects in nature. From the interesting facts about the moths, they fly at night depending on the moonlight using the mechanism of transverse orientation for navigation.

In this mechanism, the moth flies at a fixed angle with the moon which is an effective way in case of traveling a long distance in a straight path. The moths will use this mechanism and it will be efficient if the light source is far away like the moonlight. If the light source is near, the moths will not travel in a straight path, they will fly in a spiral path around the light.

There are three conditions that must be involved when using the logarithmic spiral that is described using (36) and (37) and shown in Fig 7. These conditions are as follows:

- The initial point of the spiral starts from the moth.
- The final point of the spiral is at the flame position.
- The fluctuation range of the spiral shouldn't exceed the search space.

$$S(M_i, F_j) = D_i \cdot e^{bt_x} \cdot \cos(2\pi t_x) + F_j \tag{36}$$

$$D_i = |F_j - M_i| \tag{37}$$

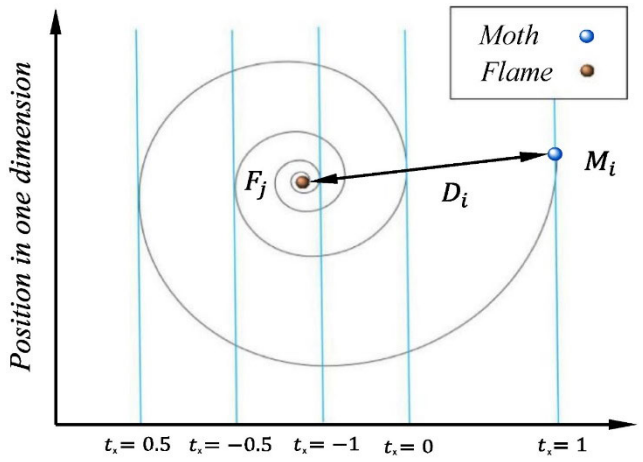

FIGURE 7. Logarithmic spiral and the position according to t_x.

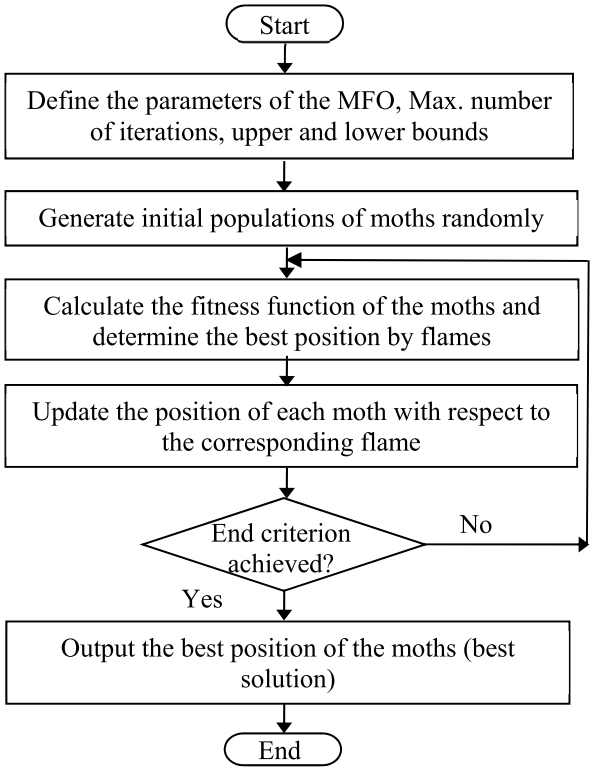

FIGURE 8. The flow chart of the MFO algorithm.

where S, M_i, F_j, t_x, b, and D_i are the logarithmic spiral of the MFO algorithm, an indication of i^{th} moth, an indication of j^{th} flame, a random number in the range $[-1,1]$, constant is used to define the logarithmic spiral shape, and distance between i^{th} moth and j^{th} flame, respectively.

In (36) and Fig. 7, the next position of the moth relative to the flame is done according to the value of the t_x parameter. $t_x = -1$ represents the closest position to the flame and $t_x = 1$ represents the farthest position to the flame.

The steps of the MFO algorithm in solving any optimization problem are shown in Fig. 8.

The steps of the MFO algorithm in solving the proposed optimization problem are summarized in the following steps:

- Defining the parameters of the MFO algorithm including the maximum number of iterations, the number of the populations, and the upper and lower bounds of the design variables (sizes of the MG resources).
- Reading the hourly WTs power, PV power, demand power, pricing of the purchased/sold power from/to the UG, time of use, and the connection status between the MG and the UG. The hourly WTs and PV powers are obtained depending on the LHS method as mentioned in step (3) in Section III-B.
- Generating the initial populations of moths randomly which represent potential solutions, calculating the fitness function of these moths (objective function) using Equations (6)-(20), and determining the best position by flames which has the lowest objective function and satisfies all the technical constraints described by Equations (21)-(35).
- Updating the position of each moth with respect to the corresponding flame using Equations (36) and (37), calculating the fitness function, and obtaining the best position same as the previous step. This step is repeated till reaching the maximum number of iterations.
- Obtaining the best position of the moths (best solution).

B. HYBRID FIREFLY and PARTICLE SWARM OPTIMIZATION (HFPSO) ALGORITHM

Several studies used the HFPSO algorithm in solving the optimization problems related to the power systems, especially the MG, and mentioned that the HFPSO obtained the best solution compared to the FA and the PSO algorithms or other techniques such as in [46], [47], and [48]. The HFPSO algorithm [46] is a metaheuristic optimization algorithm that mixes the firefly algorithm (FA) and the particle swarm optimization (PSO) algorithm to make a new robust and fast optimization technique. In HFPSO, either the PSO or the FA is used according to the type of search for the optimal solution (global or local). In the global search, the HFPSO uses the PSO because it has a fast convergence in the exploration step and it uses the FA in the local search because it has a fine-tuning in the exploitation step.

The usage of the PSO and the FA are described using (38)-(43) as follows [46]:

$$f\,(i, itr) = \begin{cases} true, if\ fitness\left(particle_i^{itr}\right) \le gbest^{itr-1} \\ false, if\ fitness\left(particle_i^{itr}\right) > gbest^{itr-1} \end{cases} \tag{38}$$

$$X_i\,(itr+1) = X_i\,(itr) + B_o e^{-\gamma r_{ij}^2}\left(X_i\,(itr) - gbest^{itr-1}\right) + a\epsilon_i \tag{39}$$

$$V_i\,(itr+1) = X_i\,(itr+1) - X_{i\_temp} \tag{40}$$

$$V_i\,(itr+1) = wV_i\,(itr) + c_1 r_1\,(pbest_i\,(itr) - X_i(itr)) + c_2 r_2\,(gbest\,(itr) - X_i(itr)) \tag{41}$$

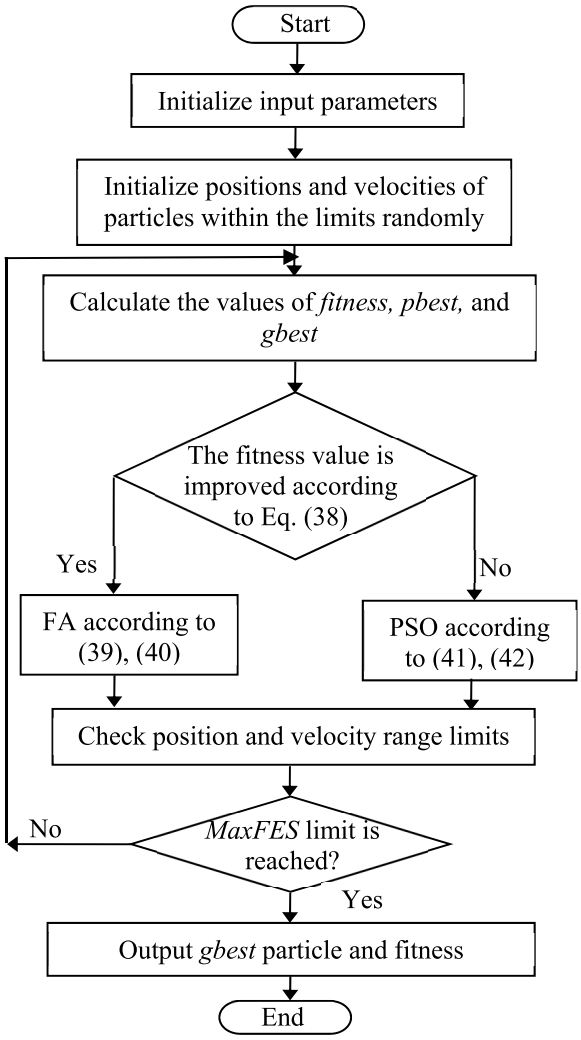

FIGURE 9. The flow chart of the HFPSO algorithm.

$$X_i\,(itr+1) = X_i\,(itr) + V_i(itr+1) \tag{42}$$

$$w = w_i - ((w_i - w_f)/itr_{max}) \times itr \tag{43}$$

where V_i and X_i are the velocity and position of ith particle or firefly, X_{i_temp} is the temporal position of ith firefly, $\gamma, B_o,$ *and* r_{ij} are the light absorption coefficient, attractiveness coefficient, and distance between two fireflies in the FA, respectively, a is random number in the range [0,1], *gbest* and *pbest* are global best particle and best particle in the PSO, respectively, r_1 and r_2 are random coefficients in the range [0,1], c_1 and c_2 are acceleration coefficients of the PSO, w is the inertia weight of the PSO, itr and itr_{max} are the current iteration and the maximum number of iterations, respectively, and *MaxFES* is the maximum number of fitness evaluations.

Equation (38) describes the comparing step between the FA and the PSO. If the fitness value of the optimization problem is improved in the last iteration, the FA is used, the current position is saved in a temporary variable $\left(X_{i_{temp}}\right)$, and a new position and velocity are calculated using (39) and (40), respectively. If the fitness value is not improved, the PSO is used, and the position and velocity are updated using (41) and (42). The steps of the HFPSO algorithm in solving any optimization problem are shown in Fig. 9.

The steps of the HFPSO algorithm in solving the proposed optimization problem are summarized in the following steps:

- Defining the parameters of the HFPSO algorithm including the maximum number of iterations, the number of populations, and the upper and lower bounds of the design variables (sizes of the MG resources).
- Reading the hourly WTs power, PV power, demand power, pricing of the purchased/sold power from/to the UG, time of use, and the connection status between the MG and the UG. The hourly WTs and PV powers are obtained depending on the LHS method as mentioned in step (3) in Section III-B.
- Generating the initial positions and velocities of the particles randomly which represent potential solutions, calculating the fitness function of these particles (objective function) using Equations (6)-(20), and determining the best particle and the global best particle which has the lowest objective function and satisfies all the technical constraints described by Equations (21)-(35).
- Improving the fitness function according to Equation (38). The improvement is done using either the FA via Equations (39) and (40) or the PSO via Equations (41) and (42). After that, checking the updated values of the position and velocity is done to be within limits. This step is repeated till reaching the maximum number of iterations.
- Obtaining the global optimal solution and its fitness value.

VI. CASE STUDIES AND RESULTS

In Table 3, the parameters of the optimization problem are included [5], [38], [49], [50], [51], [52], [53]. The types of the used WTs, PV, and Li-ion BSUs are 330 kW Italtech, Top class 500-525, and Sunverge, respectively. The MG system under study is assumed to be located at Zafarana on the Red Sea, Egypt with Latitude: 29.239^o North, Longitude: 32.598^o East, and Site altitude: 287 meters [33].

The used electricity tariffs are included in Table 4 [53]. As shown in Table 4, the on-peak time is within the hours 10-17 in the winter season, the hours 17-24 in the spring season, the hours 1 and 16-24 in the summer season, and the hours 15-22 in the fall season.

The optimization problem is implemented and solved using MATLAB software (m-file) on a computer of processor Intel(R), Core (TM), i7-4500U, CPU @1.80 GHz, and 2.4 GHz.

In this section, the results are presented and discussed as follows:

TABLE 3. Parameters of the optimization problem.

WTs and PV	
$C_{i,WT}$, $C_{i,PV}$ (\$/kW) and $C_{O,WT}$, $C_{O,PV}$ (\$/kW-year) and lifetime of WT, PV (years)	2346, 2025 and 33, 16 and 25
P_{WT}^{cap} , P_{PV}^{cap} (kW/one unit)	330, 0.5
v_{ci}, v_r, v_{co} (m/s)	3, 11.9, 25
G_{STC} (W), T_{STC} (°C), f_{PV} (%), α_T (%/°C), α_{PV} (%)	1000, 25, 85, -0.48, 80
BSUs (LI-ion Type)	
C_E (\$/kWh), C_P (\$/kW), C_O (\$/kW)	546.6, 19.8, 0
η_{ch} (%), η_{disch}(%), SOC_{min} (%), and lifetime (years)	92, 92, 10, and 10
DUs	
C_{diesel} (\$/kW) and lifetime (years)	500 and 20
a_f (\$/kW²h), b_f (\$/kWh), c_f (\$/h)	0.0002484, 0.0156, 0.3312
a_e (L/kW²h), b_e (L/kWh), c_e (L/h)	0.0001, 0.1697, 35.8
α_{CO_2}, α_{N_2O}, α_{CH_4} (kg/L) and C_{em} (\$/kg)	2.557, 0.0004, 0.000133 and 0.05
UG	
$P_{grid\ max}$ (kW)	4000
Curtailment	
$C_{dump}, C_{sh}, C_{non\ sh}$ (\$/kWh)	0.03, 0.03, 0.089
PWF	
d (%), I (years)	6, 10
Optimization problem	
W_1, W_2	0.5, 0.5
$C_{total\ max}$ (\$) and $\Delta\hat{P}_{max}$ (kW)	72788908 and 244509849
Max. no. of iterations and populations	100 and 20

TABLE 4. Electricity tariffs.

Hour	Winter (\$/kWh)	Spring (\$/kWh)	Summer (\$/kWh)	Fall (\$/kWh)
1	0.08	0.08	0.24	0.08
2	0.16	0.08	0.08	0.08
3	0.16	0.08	0.08	0.08
4	0.16	0.08	0.08	0.08
5	0.16	0.08	0.08	0.08
6	0.16	0.08	0.08	0.08
7	0.16	0.08	0.16	0.16
8	0.16	0.08	0.16	0.16
9	0.16	0.16	0.16	0.16
10	0.24	0.16	0.16	0.16
11	0.24	0.16	0.16	0.16
12	0.24	0.16	0.16	0.16
13	0.24	0.16	0.16	0.16
14	0.24	0.16	0.16	0.16
15	0.24	0.16	0.16	0.24
16	0.24	0.16	0.24	0.24
17	0.24	0.24	0.24	0.24
18	0.16	0.24	0.24	0.24
19	0.16	0.24	0.24	0.24
20	0.08	0.24	0.24	0.24
21	0.08	0.24	0.24	0.24
22	0.08	0.24	0.24	0.24
23	0.08	0.24	0.24	0.08
24	0.08	0.24	0.24	0.08

- First, three case studies are presented to illustrate the system policy and the role of the multi-functional BSUs in different MG operating conditions.
- Second, three case studies are presented to show the importance of considering the stochastic behavior of different parameters and the DSM in the proposed methodology.
- Third, two case studies are presented to show the effect of changing the percentage of the fixed loads in the DSM on the optimal sizing of the MG.
- Finally, a comparison is presented between the used two metaheuristic optimization algorithms, MFO and HFPSO, to show their ability in solving the proposed optimization problem and to assure the optimal solution.

A. DIFFERENT OPERATING CONDITIONS OF THE MG

There are 100 scenarios of one year as mentioned before in Section III-B. As an example, three sample days are chosen from the study period to illustrate the system policy and the role of the multi-functional BSUs in different MG operating conditions. The sample days represent three different cases of the generation from the RESs compared to the demand as follows:

- First sample day (S1), the generation from the RESs $\leq$ the demand.
- Second sample day (S2), the generation from the RESs $\geq\leq$ the demand. However, in this sample day, the hours with power deficit $>$ the hours with surplus power.
- Third sample day (S3), the generation from the RESs $\geq\leq$ the demand. However, in this sample day, the hours with power deficit $<$ the hours with surplus power.

Fig. 10 shows the power patterns of the three selected samples including the generation from the RESs, the demand before the DSM, the demand after the DSM, the BSUs, the UG, and the DUs, respectively. In Fig. 10(d), if the power of the BSUs is positive, the BSUs are charged and vice versa. Also, in Fig. 10(e), if the power of the UG is positive, this power represents sold power from the MG to the UG. If the power of the grid is negative, this power represents purchased power from the UG to the MG.

From the power figures, the following observations can be recorded:

1) OPERATION OF THE BSUs

As shown in Fig. 10(d), the BSUs do the following functions on the first sample day (S1):

- Function 1 (generation/demand matching): The BSUs are discharged at hours 5 and 6 to satisfy the power deficit from the RESs.
- Function 2 (energy arbitrage): There are two times of energy arbitrage within the selected day. The first one is done during hours 7, 8, 10, and 11 as the BSUs are charged at hours 7 and 8 (off-peak time) and discharged at hours 10 and 11 (on-peak time) because the on-peak time in this sample is within the hours 10-17. The second

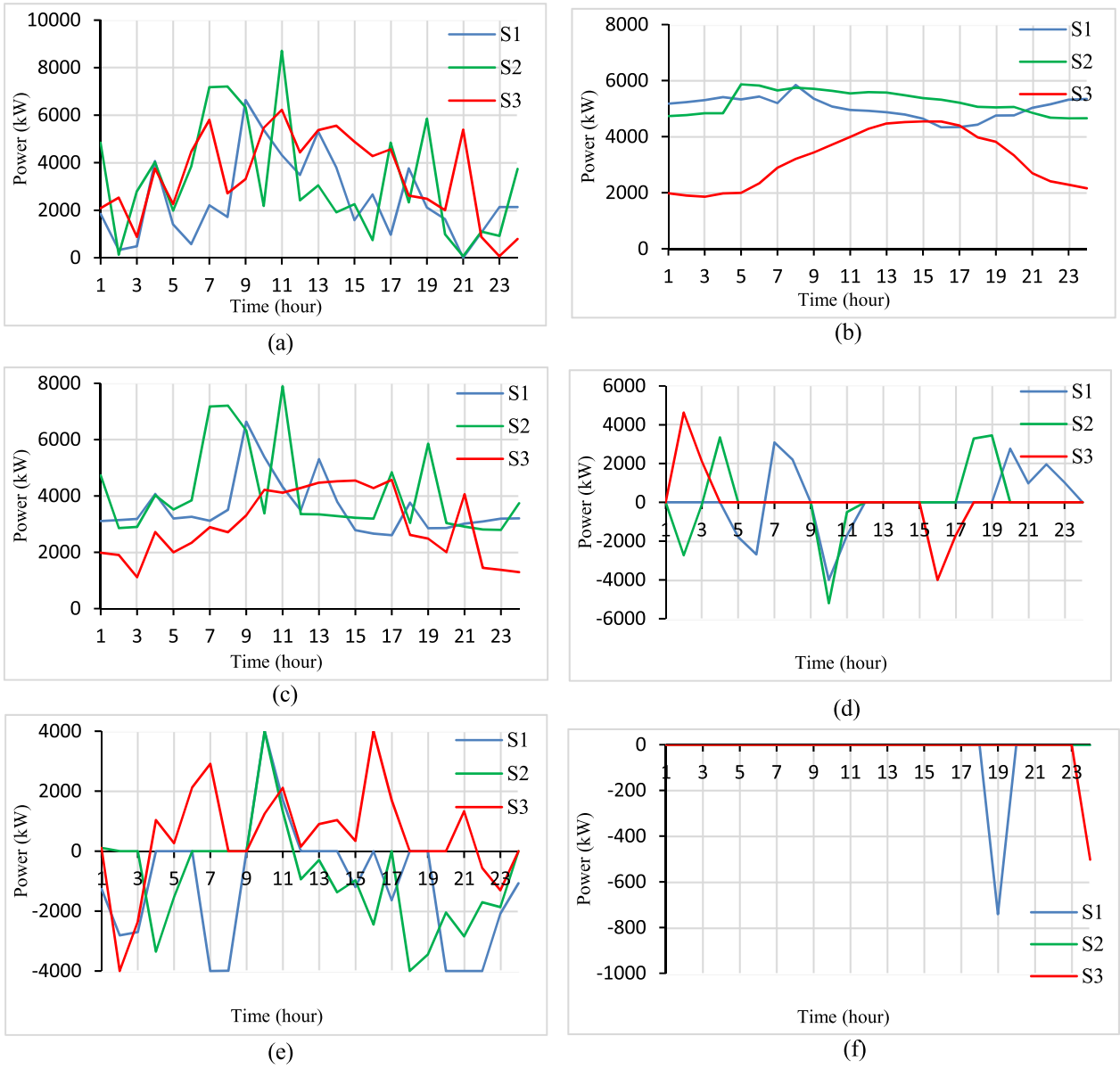

FIGURE 10. The power figures of the selected three sample days include; (a) total power generation from the RESs, (b) demand power before the DSM, (c) demand power after the DSM, (d) BSUs power, (e) UG power, and (f) DUs power.

time is done during hours 20-23 as the BSUs are charged at hours 20-23 (off-peak time), but the BSUs are not discharged as no other on-peak time is available till the end of this day.

On the second sample day (S2), the BSUs do the following functions:

- Function 1 (generation/demand matching): The BSUs are discharged at hours 2, 3, and 10 to satisfy the power deficit from the RESs.
- Function 2 (energy arbitrage): There are two times of energy arbitrage within the selected day. The first one is done during hours 4, 10, and 11 as the BSUs are charged at hour 4 (off-peak time) and discharged at hours 10 and 11 (on-peak time) because the on-peak time in this sample is within hours 10-17. The second time is done during hours 18 and 19 as the BSUs are charged at hours 18 and 19 (off-peak time), but the BSUs are not discharged as no other on-peak time is available till the end of this day. As shown, the BSUs perform the two functions together at hour 10.

On the third sample day (S3), the BSUs do the following functions:

- Function 1 (generation/demand matching): The BSUs are charged at hour 2 from the surplus power from the RESs.
- Function 2 (energy arbitrage): There is only one time of energy arbitrage during hours 2, 3, 16, and 17 within the selected day as the BSUs are charged at hours 2 and 3

(off-peak time) and discharged at hours 16 and 17 (on-peak time) because the on-peak time in this sample is within hours 1 and 16-24. As shown, the BSUs perform the two functions together at hour 2.

2) OPERATION OF THE DUs

On the first sample day (S1), the MG is disconnected from the UG within hours 5, 6, 18, and 19. As shown in Fig. 10(f), the DUs supply the demand during hour 19 to cover the power deficit because the MG is islanded and the BSUs are empty.

On the second sample day (S2), the MG is disconnected from the UG within hours 2, 3, and 24. As shown in Fig. 10(f), the DUs don't supply the demand during any hour of the day.

On the third sample day (S3), the MG is disconnected from the UG at hour 24. As shown in Fig. 10(f), the DUs supply the demand during hour 24 to cover the power deficit because the MG is islanded and the BSUs are empty.

3) POWER TRANSFER WITH THE UG

As shown in Fig. 10(e), the purchased/sold power from/to the UG on the first sample day (S1) occurs as follows:

- The power is purchased from the UG during hours 1-3, 7, 8, 15, 17, and 20-24 to cover the power deficit and during hours 7, 8, and 20-23 to be used for the energy arbitrage.
- The power is sold to the UG during hours 10 and 11 due to the energy arbitrage process.

On the second sample day (S2), the purchased/sold power from/to the UG occurs as follows:

- The power is purchased from the UG during hours 5, 12-16, 18, and 20-23 to cover the power deficit and during hours 4, 18, and 19 to be used for the energy arbitrage.
- The power is sold to the UG during hours 1 and 11 from the surplus power from the RESs and during hours 10 and 11 due to the energy arbitrage process.

On the third sample day (S3), the purchased/sold power from/to the UG occurs as follows:

- The power is purchased from the UG during hours 3, 22, and 23 to cover the power deficit and during hours 2 and 3 to be used for the energy arbitrage.
- The power is sold to the UG during hours 1, 4-7, 10-15, and 21 from the surplus power of the RESs and during hours 16 and 17 to be used for the energy arbitrage.

4) TYPES OF DEMAND

As shown in Fig. 10(a)-(c), the three types of demand occur on the first sample day (S1) as follows:

- The ED occurs during hours 9, 10, and 13.
- The PSCD occurs during hours 1-3 as a part of the demand is shifted from hours 1, 2, and 3 to hours 9, 10, and 13 (total shifted demand = 2026 kW from total unsupplied demand = 6289 kW), respectively.
- The PCD occurs during hours 4-8, 11, 12, and 14-24 (total curtailed demand = 31205 kW).

On the second sample day (S2), the three types of demand occur as follows:

- The ED occurs during hours 1, 7-9, 11, and 19.
- The PSCD occurs during hours 2-6 as a part of the demand is shifted from hours 2-6 to hours 7-9, 11, and 19 (total shifted demand = 6759 kW from total unsupplied demand = 8979 kW), respectively.
- The PCD occurs during hours 10, 12-18, and 20-24 (total curtailed demand = 24205 kW).

On the third sample day (S3), the three types of demand occur as follows:

- The ED occurs during hours 1, 2, 4-7, 10-15, 17, and 21.
- The PSCD occurs during hours 3, 8, 9, 16, and 18 as a part of the demand is shifted from hours 3, 8, 9, 16, and 18 to hours 4, 10, 11, 17, and 21 (total shifted demand = 2895 kW from total unsupplied demand = 2986 kW), respectively.
- The PCD occurs during hours 19, 20, and 22-24 (total curtailed demand = 5407 kW).

5) CASES RELATED TO THE GENERATION AND DEMAND

On the first sample day (S1), the hours of the system policy cases are as follows:

- Case 1 occurs during hours 4 and 9.
- Case 2 occurs during hours 10-14 and 16.
- Case 3 occurs during hours 1-3, 7, 8, and 20-24.
- Case 4 occurs during hours 15 and 17.
- Case 5 occurs during hours 18.
- Case 6 occurs during hours 5, 6, and 19.

On the second sample day (S2), the hours of the system policy cases are as follows:

- Case 1 occurs during hours 1, 4, 6-9, and 19.
- Case 2 occurs during hours 11 and 17.
- Case 3 occurs during hours 5, 18, and 20-23.
- Case 4 occurs during hours 10 and 12-16.
- Case 5 occurs during hours 24.
- Case 6 occurs during hours 2 and 3.

On the third sample day (S3), the hours of the system policy cases are as follows:

- Case 1 occurs during hours 2 and 4-15.
- Case 2 occurs during hours 1 and 16-21.
- Case 3 occurs during hour 3.
- Case 4 occurs during hours 22 and 23.
- Case 5 doesn't exist.
- Case 6 occurs during hour 24.

After comparing the three sample days (S1, S2, and S3), the following points which are related to the operation of the MG components and the UG can be concluded:

- The hours of the BSUs operation are the highest on the first sample day (10 hours) and lowest on the third sample day (4 hours). As a result, the operation of the BSUs increases as the power deficit increases during the hours of the day. This reflects the important role of the BSUs in the MG to enhance the MG performance.

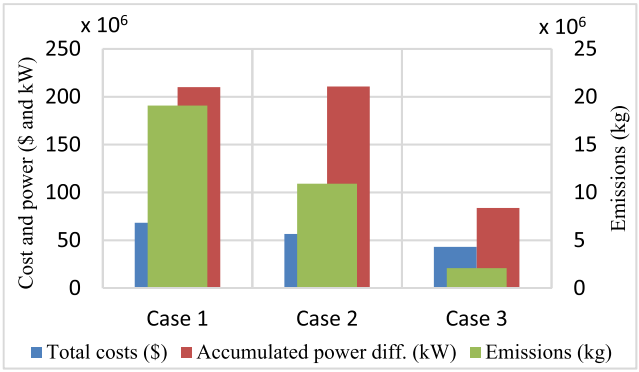

FIGURE 11. Deterministic and stochastic case studies.

- The DUs operate according to the status of the BSUs and the power deficit from the RESs during the islanding hours of the MG. As an example, the DUs supply the demand during one hour of the islanding hours on the first sample day because the BSUs are empty during this islanding hour. However, the BSUs cover the power deficit during the other islanding hours on this day.
- With respect to the power transfer with the UG, the power selling to the UG increases as the power surplus from the RESs and the energy arbitrage (on-peak time) increase. As a result, the highest power selling occurs on the third sample day (14 hours) and the lowest power selling occurs on the first sample day (2 hours). On the other hand, the power purchasing from the UG increases as the power deficit from the RESs and the energy arbitrage (off-peak time) increase. As a result, the highest power purchasing occurs on the first sample day (12 hours) and the lowest power purchasing occurs on the third sample day (5 hours).
- With respect to the demand curtailment, the curtailment of the demand is the highest on the first sample day and lowest on the third sample day. As a result, it increases with the increase of the power deficit from the RESs during the hours of the day.

B. DETERMINISTIC VS. STOCHASTIC AND IMPACT OF THE DSM

Three case studies are presented to investigate the need of considering the stochastic behavior of different parameters, as well as considering the DSM in the proposed work. These cases are as follows:

- Case 1: uses the deterministic model without considering the DSM.
- Case 2: uses the stochastic model without considering the DSM.
- Case 3: considers the stochastic model and the DSM.

Table 5 and Fig. 11 show the optimal sizing of the MG for the three case studies and show the effect of each case study on the three main objectives of the proposed work.

TABLE 5. Results of the three case studies.

		Case 1	Case 2	Case 3
N_{WT}	No. of units	30	31	22
N_{PV}	No. of units	7836	5977	5080
E_B^{cap}, P_B^{cap}	kWh, kW	6371, 6232.5	9999, 9781.6	6893, 6743.2
P_{diesel}^{cap}	kW	7024.7	6956.5	3781.8
C_{total}	(x10^6) $	68.2	56.6	43.1
	p.u.	0.9368	0.7775	0.5925
C_{em}	(x10^6) kg	19.1	10.9	2.1
	(x10^6) $	0.953	0.546	0.105
	p.u.	0.0131	0.0075	0.0014
$\Delta\hat{P}$	(x10^6) kW	209.9	210.7	83.7
	p.u.	0.8586	0.8617	0.3425
obj	p.u.	0.8977	0.8196	0.4675

TABLE 6. Results of changing the percentage of the fixed loads.

		30%	60%
N_{WT}	No. of units	16	22
N_{PV}	No. of units	4332	5080
E_B^{cap}, P_B^{cap}	kWh, kW	1076, 1052.6	6893, 6743.2
P_{diesel}^{cap}	kW	1899.3	3781.8
C_{total}	(x10^6) $	36.8	43.1
	p.u.	0.5067	0.5925
C_{em}	(x10^6) kg	0.79	2.1
	(x10^6) $	0.039	0.105
	p.u.	0.0005 p.u.	0.0014
$\Delta\hat{P}$	(x10^6) kW	26.7	83.7
	p.u.	0.1094	0.3425
obj	p.u.	0.3081	0.4675

To show the effect of considering the stochastic behavior of different parameters without considering the DSM, the results of the first and second cases are compared. As shown in Table 5 and Fig. 11, there are noticeable differences between the total costs and the harmful gas emissions and a very small difference between the total accumulated power difference for the two cases. Furthermore, the results of the second case are considered more accurate because it reflects the stochastic behavior of the uncertain parameters in the proposed methodology.

To show the effect of considering the DSM with the stochastic model, the results of the second and third cases are compared. As shown in Table 5 and Fig. 11, considering the DSM in the third case (proposed methodology) reduces the total costs of the MG, the harmful gas emissions, and the total accumulated power difference. In the third case, the total costs are reduced by 13.5×10^6 $ (23.9%), the emissions are

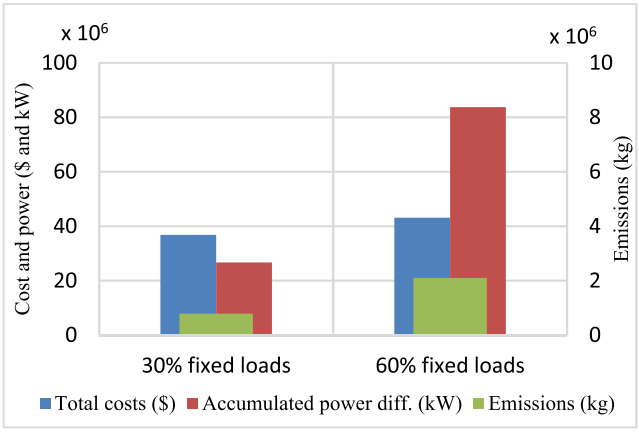

FIGURE 12. 30% and 60% fixed loads in the DSM.

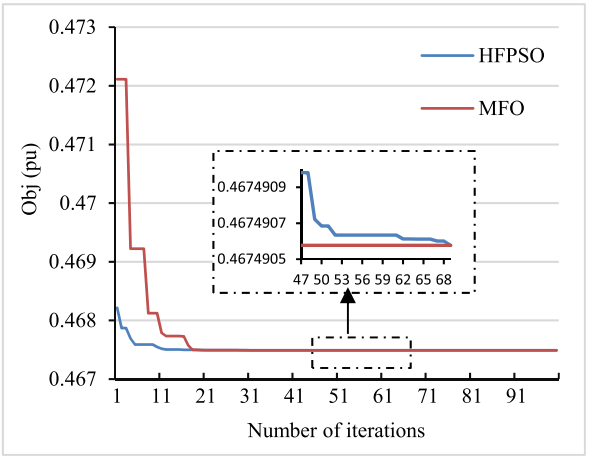

FIGURE 13. Convergence curve of the MFO and the HFPSO.

reduced by 8.8×10^6 kg (80.7%), and the accumulated power difference is reduced by 127×10^6 kW (60.3%).

Thus, considering both the uncertainties and the DSM in the proposed methodology leads to the best accurate results.

C. EFFECT OF CHANGING THE PERCENTAGE OF THE FIXED LOADS IN THE DSM

The percentage of the fixed loads has no fixed value but is decided based on the system policy and agreement with the customers. In this subsection, the effect of changing the percentage of the fixed loads (30% and 60%) on the optimal sizing of the MG and the values of the three objectives are shown in Table 6 and Fig. 12.

As shown in Table 6 and Fig. 12, increasing the percentage of the fixed loads in the DSM leads to an increase in the total costs of the MG, the harmful gas emissions, and the total accumulated power difference. As shown, the change in this percentage affects slightly the total costs and the harmful gas emissions. However, the accumulated power difference is more affected, so the optimal sizing of the MG is increased to cover this change in the accumulated power difference between the generation from the RESs and the demand.

D. COMPARISON BETWEEN HFPSO AND MFO

In this subsection, the ability of the used metaheuristic optimization algorithms, MFO and HFPSO, in solving the proposed optimization problem is presented. As a result of multiple runs of the MATLAB software, the optimal solution of the proposed optimization problem using the MFO and the HFPSO is presented in Table 7. Fig. 13 shows the convergence curve of the MFO and HFPSO techniques.

From Table 7 and Fig. 13, it is noticed that the obtained optimal solution is the same for the MFO and the HFPSO, but the MFO converges faster than the HFPSO. This reflects that the obtained solution from the two techniques is considered the global optimal solution. Fig. 13 shows that the used optimization techniques (MFO and HFPSO) are considered robust methodologies. This is due to the two techniques that can reach the global optimal solution with a few iterations

TABLE 7. Results of the optimization problem using MFO and HFPSO.

		HFPSO	MFO
N_{WT}, N_{PV}	unit	22, 5080	22, 5080
E_B^{cap}, P_B^{cap}	kWh, kW	6893, 6743.2	6893, 6743.2
P_{diesel}^{cap}	kW	3781.8	3781.8
C_{total}	$	43125473.74	43125473.74
	pu	0.5924732	0.5924732
$\Delta\hat{P}$	kW	83746579.82	83746579.82
	pu	0.3425080	0.3425080
obj	pu	0.4674905	0.4674905

(lower than 100 iterations) despite the complexity of the proposed optimization problem. The figure also shows that the number of iterations of the MFO to reach the optimal solution (47 iterations) is lower than HFPSO (69 iterations). This proves that the MFO technique is better than the HFPSO technique in solving the proposed optimization problem with respect to the speed to reach the optimal solution.

VII. CONCLUSION

An effective MG planning methodology is presented in this paper which allows the BSUs to perform multi-function. The functions considered in this study are supply/demand matching and energy arbitrage. The first function (supply/demand matching) is to store the surplus power during the high-power time of the generation from the RESs and cover the deficit during the low-power time of the generation from the RESs. The second function (energy arbitrage) is to purchase the power from the UG during the off-peak time (low price) and sell it again during the on-peak time (high price) resulting in a profit. The obtained optimal sizing of the MG resources including the RESs/BSUs/DUs enhances the performance of the MG system. This is achieved by minimizing the total costs of the MG, the harmful gas emissions, and the accumulated power difference between the generation from the RESs and

the demand. To obtain realistic results, the uncertainties of several parameters such as wind speed, solar irradiance, and temperature are considered in the study. In addition, the two modes of operation of the MG (grid-connected and islanded) and the DSM are also considered. The results show the ability of the proposed system policy to operate the MG efficiently under different operating conditions to ensure achieving profits for the MG. Moreover, the benefits obtained from installing BSUs are maximized due to their multi-functional operation. The results of the different case studies show that considering the uncertainties and the DSM with the aid of the multi-functional BSUs in the proposed methodology leads to accurate results while achieving benefits to the system owner. The results also show that the optimal sizing of the MG is affected by the percentage of fixed loads in the DSM. Finally, a comparison is done between the two used metaheuristic optimization algorithms, MFO and HFPSO, to assure the optimal solution and show their robustness in solving the proposed constrained nonlinear problem. This comparison shows that the same optimal solution is obtained, but the MFO algorithm is better than the HFPSO algorithm with respect to the speed to reach this optimal solution.

To apply the proposed methodology in a real microgrid scenario, different factors should be considered in the offline procedure of the planning phase. These factors include the limitations with respect to the geographical location of the MG which can affect the number of installed units. Also, the methodology requires accurate historical data on the weather and demand. The electricity pricing scheme specified by the utility operator is also an important factor to be considered. In addition to the accurate coefficients related to harmful gas emissions based on environmental constraints.

VIII. FUTURE WORK

The proposed methodology can be extended to include the following points in future studies:

- Use of different types of energy storage systems at different time scales.
- Performing different functions than those considered in this study, such as stability and power quality enhancement of the MG.
- Studying load demand forecasting in urban community cluster MGs using machine learning methods.

REFERENCES

[1] B. Papari, C. S. Edrington, I. Bhattacharya, and G. Radman, "Effective energy management of hybrid AC-DC microgrids with storage devices," *IEEE Trans. Smart Grid*, vol. 10, no. 1, pp. 193–203, Jan. 2019.

[2] I. Alsaidan, A. Khodaei, and W. Gao, "A comprehensive battery energy storage optimal sizing model for microgrid applications," *IEEE Trans. Power Syst.*, vol. 33, no. 4, pp. 3968–3980, Jul. 2018.

[3] M. Al-Saadi, M. Al-Greer, and M. Short, "Strategies for controlling microgrid networks with energy storage systems: A review," *Energies*, vol. 14, no. 21, p. 7234, Nov. 2021.

[4] M. Faisal, M. A. Hannan, P. J. Ker, A. Hussain, M. B. Mansor, and F. Blaabjerg, "Review of energy storage system technologies in microgrid applications: Issues and challenges," *IEEE Access*, vol. 6, pp. 35143–35164, 2018.

[5] U. Akram, M. Khalid, and S. Shafiq, "An innovative hybrid wind-solar and battery-supercapacitor microgrid system-development and optimization," *IEEE Access*, vol. 5, pp. 25897–25912, 2017.

[6] O. Ouramdane, E. Elbouchikhi, Y. Amirat, and E. S. Gooya, "Optimal sizing of domestic grid-connected microgrid maximizing self consumption and battery lifespan," *IFAC-PapersOnLine*, vol. 55, no. 12, pp. 683–688, 2022.

[7] S. Bandyopadhyay, G. R. C. Mouli, Z. Qin, L. R. Elizondo, and P. Bauer, "Techno-economical model based optimal sizing of PV-battery systems for microgrids," *IEEE Trans. Sustain. Energy*, vol. 11, no. 3, pp. 1657–1668, Jul. 2020.

[8] R. Atia and N. Yamada, "Sizing and analysis of renewable energy and battery systems in residential microgrids," *IEEE Trans. Smart Grid*, vol. 7, no. 3, pp. 1204–1213, May 2016.

[9] U. Akram, M. Khalid, and S. Shafiq, "Optimal sizing of a wind/solar/battery hybrid grid-connected microgrid system," *IET Renew. Power Gener.*, vol. 12, no. 1, pp. 72–80, Aug. 2018.

[10] R. Garmabdari, M. Moghimi, F. Yang, E. Gray, and J. Lu, "Multi-objective energy storage capacity optimisation considering microgrid generation uncertainties," *Int. J. Electr. Power Energy Syst.*, vol. 119, Jul. 2020, Art. no. 105908.

[11] L. Bhamidi and S. Sivasubramani, "Optimal planning and operational strategy of a residential microgrid with demand side management," *IEEE Syst. J.*, vol. 14, no. 2, pp. 2624–2632, Jun. 2020.

[12] M. Kharrich, S. Kamel, M. Abdeen, O. H. Mohammed, M. Akherraz, T. Khurshaid, and S.-B. Rhee, "Developed approach based on equilibrium optimizer for optimal design of hybrid PV/wind/diesel/battery microgrid in Dakhla, Morocco," *IEEE Access*, vol. 9, pp. 13655–13670, 2021.

[13] İ. Cetinbaş, B. Tamyürek, and M. Demırtaş, "The hybrid Harris hawks optimizer-arithmetic optimization algorithm: A new hybrid algorithm for sizing optimization and design of microgrids," *IEEE Access*, vol. 10, pp. 19254–19283, 2022.

[14] A. A. Z. Diab, H. M. Sultan, I. S. Mohamed, O. N. Kuznetsov, and T. D. Do, "Application of different optimization algorithms for optimal sizing of PV/wind/diesel/battery storage stand-alone hybrid microgrid," *IEEE Access*, vol. 7, pp. 119223–119245, 2019.

[15] B. Li, R. Roche, and A. Miraoui, "Microgrid sizing with combined evolutionary algorithm and MILP unit commitment," *Appl. Energy*, vol. 188, pp. 547–562, Feb. 2017.

[16] M. Kumar and B. Tyagi, "Multi-variable constrained non-linear optimal planning and operation problem for isolated microgrids with stochasticity in wind, solar, and load demand data," *IET Gener., Transmiss. Distribut.*, vol. 14, no. 11, pp. 2181–2190, Jun. 2020.

[17] B. Ismail, N. I. A. Wahab, M. L. Othman, M. A. M. Radzi, K. N. Vijyakumar, and M. N. M. Naain, "A comprehensive review on optimal location and sizing of reactive power compensation using hybrid-based approaches for power loss reduction, voltage stability improvement, voltage profile enhancement and loadability enhancement," *IEEE Access*, vol. 8, pp. 222733–222765, 2020.

[18] H. Kang, R. Liu, Y. Yao, and F. Yu, "Improved Harris hawks optimization for non-convex function optimization and design optimization problems," *Math. Comput. Simul.*, vol. 204, pp. 619–639, Feb. 2023.

[19] T. Bhattacharyya, B. Chatterjee, P. K. Singh, J. H. Yoon, Z. W. Geem, and R. Sarkar, "Mayfly in harmony: A new hybrid meta-heuristic feature selection algorithm," *IEEE Access*, vol. 8, pp. 195929–195945, 2020.

[20] Y. Meraihi, A. B. Gabis, A. Ramdane-Cherif, and D. Acheli, "A comprehensive survey of crow search algorithm and its applications," *Artif. Intell. Rev.*, vol. 54, no. 4, pp. 2669–2716, Apr. 2021.

[21] P. Agrawal, H. F. Abutarboush, T. Ganesh, and A. W. Mohamed, "Metaheuristic algorithms on feature selection: A survey of one decade of research (2009–2019)," *IEEE Access*, vol. 9, pp. 26766–26791, 2021.

[22] B. Khan and P. Singh, "Selecting a meta-heuristic technique for smart micro-grid optimization problem: A comprehensive analysis," *IEEE Access*, vol. 5, pp. 13951–13977, 2017.

[23] S. E. De León-Aldaco, H. Calleja, and J. A. Alquicira, "Metaheuristic optimization methods applied to power converters: A review," *IEEE Trans. Power Electron.*, vol. 30, no. 12, pp. 6791–6803, Dec. 2015.

[24] S. Lalljith, I. Fleming, U. Pillay, K. Naicker, Z. J. Naidoo, and A. K. Saha, "Applications of flower pollination algorithm in electrical power systems: A review," *IEEE Access*, vol. 10, pp. 8924–8947, 2022.

[25] Z. Zheng, S. Yang, Y. Guo, X. Jin, and R. Wang, "Meta-heuristic techniques in microgrid management: A survey," *Swarm Evol. Comput.*, vol. 78, Apr. 2023, Art. no. 101256.

[26] M. Fathi, R. Khezri, A. Yazdani, and A. Mahmoudi, "Comparative study of metaheuristic algorithms for optimal sizing of standalone microgrids in a remote area community," *Neural Comput. Appl.*, vol. 34, no. 7, pp. 5181–5199, Jun. 2021.
[27] D. Fioriti, D. Poli, P. Duenas-Martinez, and A. Micangeli, "Multiple design options for sizing off-grid microgrids: A novel single-objective approach to support multi-criteria decision making," *Sustain. Energy, Grids Netw.*, vol. 30, Jun. 2022, Art. no. 100644.
[28] S. Panda, S. Mohanty, P. K. Rout, B. K. Sahu, M. Bajaj, H. M. Zawbaa, and S. Kamel, "Residential demand side management model, optimization and future perspective: A review," *Energy Rep.*, vol. 8, pp. 3727–3766, Nov. 2022.
[29] L. Chu, E. S. De Cursi, A. El Hami, and M. Eid, "Application of Latin hypercube sampling based Kriging surrogate models in reliability assessment," *Sci. J. Appl. Math. Statist.*, vol. 3, no. 6, pp. 263–274, 2015.
[30] Z. Wang, Y. Chen, S. Mei, S. Huang, and Y. Xu, "Optimal expansion planning of isolated microgrid with renewable energy resources and controllable loads," *IET Renew. Power Gener.*, vol. 11, no. 7, pp. 931–940, Jul. 2017.
[31] J. Menčík, "Latin hypercube sampling," in *Concise Reliability for Engineers*. London, U.K.: IntechOpen, 2016. [Online]. Available: https://www.intechopen.com/chapters/50120
[32] H. Zhu, S. Yuan, and C. Li, "Stochastic economic dispatching strategy of the active distribution network based on comprehensive typical scenario set," *IEEE Access*, vol. 8, pp. 201147–201157, 2020.
[33] *MERRA-2 tavg_2D_slv_Nx: 2D, 1-Hourly, Time-Averaged, Single-Level, Assimilation, Single-Level Diagnostics V5.12.4*, Goddard Earth Sci. Data, Inf. Services Center (GES DISC), Global Model. Assimilation Office (GMAO), Greenbelt, MD, USA, 2015. Accessed: Dec. 2020. [Online]. Available: http://www.soda-pro.com/web-services/meteo-data/merra, doi: 10.5067/VJAFPLI1CSIV.
[34] P. Machado, R. S. Netto, L. E. Souza, and J. Maun, "Probabilistic and multi-objective approach for planning of microgrids under uncertainty: A distributed architecture proposal," *IET Gener., Transmiss. Distrib.*, vol. 13, no. 7, pp. 1025–1035, Apr. 2019.
[35] M. Manohar, E. Koley, and S. Ghosh, "Microgrid protection under weather uncertainty using joint probabilistic modeling of solar irradiance and wind speed," *Comput. Electr. Eng.*, vol. 86, Sep. 2020, Art. no. 106684.
[36] A. Stahel, *Octave and MATLAB for Engineering Applications*. Wiesbaden, Germany: Springer, 2022. Accessed: Dec. 25, 2022.
[37] M. Erdenebat, B. Galsan, H. Shuang, and M. Chimed, "Wind energy resource assessment of the south Gobi region in Mongolia," in *Proc. IEEE Region 10 Symp. (TENSYMP)*, Jun. 2020, pp. 535–538.
[38] M. S. Taha and Y. A.-R.-I. Mohamed, "Robust MPC-based energy management system of a hybrid energy source for remote communities," in *Proc. IEEE Electr. Power Energy Conf. (EPEC)*, Ottawa, ON, Canada, Oct. 2016, pp. 1–6.
[39] M. Ahmed, L. Meegahapola, A. Vahidnia, and M. Datta, "Stability and control aspects of microgrid architectures–A comprehensive review," *IEEE Access*, vol. 8, pp. 144730–144766, 2020.
[40] N. Kang, J. Wang, R. Singh, and X. Lu, "Interconnection, integration, and interactive impact analysis of microgrids and distribution systems," Argonne Nat. Lab. (ANL), Argonne, IL, USA, Tech. Rep. ANL/ESD-17/4134097, 2017, doi: 10.2172/1349056.
[41] S. Mohseni and A. C. Brent, "Economic viability assessment of sustainable hydrogen production, storage, and utilisation technologies integrated into on- and off-grid micro-grids: A performance comparison of different metaheuristics," *Int. J. Hydrogen Energy*, vol. 45, no. 59, pp. 34412–34436, Dec. 2020.
[42] S. Mohseni, A. C. Brent, and D. Burmester, "A comparison of metaheuristics for the optimal capacity planning of an isolated, battery-less, hydrogen-based micro-grid," *Appl. Energy*, vol. 259, Feb. 2020, Art. no. 114224.
[43] S. Mohseni, A. C. Brent, and D. Burmester, "A demand response-centred approach to the long-term equipment capacity planning of grid-independent micro-grids optimized by the moth-flame optimization algorithm," *Energy Convers. Manage.*, vol. 200, Nov. 2019, Art. no. 112105.
[44] S. Mirjalili, "Moth-flame optimization algorithm: A novel nature-inspired heuristic paradigm," *Knowl.-Based Syst.*, vol. 89, pp. 228–249, Nov. 2015.
[45] M. Shehab, L. Abualigah, H. A. Hamad, H. Alabool, M. Alshinwan, and A. M. Khasawneh, "Moth-flame optimization algorithm: Variants and applications," *Neural Comput. Appl.*, vol. 32, no. 14, pp. 9859–9884, 2020.
[46] I. M. Ibrahim, W. A. Omran, and A. Y. Abdelaziz, "Optimal sizing of microgrid system using hybrid firefly and particle swarm optimization algorithm," in *Proc. 22nd Int. Middle East Power Syst. Conf. (MEPCON)*. Asyut, Egypt: Assiut Univ., Dec. 2021, pp. 287–293.
[47] P. K. Ray and A. Mohanty, "A robust firefly–swarm hybrid optimization for frequency control in wind/PV/FC based microgrid," *Appl. Soft Comput.*, vol. 85, Dec. 2019, Art. no. 105823.
[48] J. S. J. Malar, A. B. Beevi, and M. Jayaraju, "Efficient power flow management in hybrid renewable energy systems," *IETE J. Res.*, vol. 69, no. 2, pp. 1088–1100, 2020.
[49] L. Xu, X. Ruan, C. Mao, B. Zhang, and Y. Luo, "An improved optimal sizing method for wind-solar-battery hybrid power system," *IEEE Trans. Sustain. Energy*, vol. 4, no. 3, pp. 774–785, Jul. 2013.
[50] A. A. Kebede, T. Coosemans, M. Messagie, T. Jemal, H. A. Behabtu, J. Van Mierlo, and M. Berecibar, "Techno-economic analysis of lithium-ion and lead-acid batteries in stationary energy storage application," *J. Energy Storage*, vol. 40, Aug. 2021, Art. no. 102748.
[51] W.-T. Huang, K.-C. Yao, and C.-C. Wu, "Using the direct search method for optimal dispatch of distributed generation in a medium-voltage microgrid," *Energies*, vol. 7, no. 12, pp. 8355–8373, Dec. 2014.
[52] A. Conteh, M. E. Lotfy, K. M. Kipngetich, T. Senjyu, P. Mandal, and S. Chakraborty, "An economic analysis of demand side management considering interruptible load and renewable energy integration: A case study," *Sustainability*, vol. 11, no. 10, p. 2828, May 2019.
[53] R. Hemmati, H. Mehrjerdi, and M. Bornapour, "Hybrid hydrogen-battery storage to smooth solar energy volatility and energy arbitrage considering uncertain electrical-thermal loads," *Renew. Energy*, vol. 154, pp. 1180–1187, Jul. 2020.

IBRAHIM M. IBRAHIM received the B.Sc. and M.Sc. degrees in electrical engineering from Ain Shams University, Cairo, Egypt, in 2011 and 2018, respectively, where he is currently pursuing the Ph.D. degree with the Department of Electrical Power and Machines, Faculty of Engineering. He is also a Teacher Assistant with the Department of Electrical Power and Machines, Faculty of Engineering, Ain Shams University. His research interests include the planning and operation of microgrids, renewable energy integration, and energy storage systems.

ALMOATAZ Y. ABDELAZIZ (Senior Member, IEEE) received the Ph.D. degree in electrical engineering according to the channel system between Ain Shams University and Brunel University, U.K., in 1996. He has been a Professor of electrical power engineering with Ain Shams University, since 2007. He has authored or coauthored more than 450 refereed journals and conference papers, 45 book chapters, and six edited books with Elsevier, Springer, and CRC Press. In addition, he has supervised more than 80 master's and 35 Ph.D. theses. His research interests include the applications of artificial intelligence and evolutionary and heuristic optimization techniques to power system planning, operation, and control. He is a member of the Egyptian Subcommittees of IEC and CIGRE. He has received many prizes for distinct research work and international publishing from Ain Shams University and Future University in Egypt. He is the Chair of the IEEE Education Society Chapter, Egypt. He is an Editor of *Electric Power Components and Systems*. He is an editorial board member, an editor, an associate editor, and an editorial advisory board member of many international journals.

HASSAN HAES ALHELOU (Senior Member, IEEE) received the B.Sc. degree (Hons.) from Tishreen University, Syria, in 2011, and the M.Sc. and Ph.D. degrees (Hons.) from the Isfahan University of Technology (IUT), Iran.

He is currently with the Department of Electrical and Computer Systems Engineering, Monash University, Clayton, VIC, Australia. He is also a Professor and a Faculty Member with Tishreen University and a Consultant with Sultan Qaboos University (SQU), Oman. Previously, he was with the School of Electrical and Electronic Engineering, University College Dublin (UCD), Dublin, Ireland, from 2020 to 2021. He was also with IUT. He has participated in more than 15 international industrial projects across the globe. His research articles received more than 3000 citations with an H-index of 29 and an i-index of 67. He has authored/edited 15 books published by reputed publishers, such as Springer, IET, Wiley, Elsevier, and Taylor & Francis. He has published more than 200 research papers in high-quality peer-reviewed journals and international conferences. His major research interests include renewable energy systems, power systems, power system security, power system dynamics, power system cybersecurity, power system operation, control, dynamic state estimation, frequency control, smart grids, microgrids, demand response, and load shedding. He was a recipient of the Outstanding Reviewer Award from many journals, such as *Energy Conversion and Management* (ECM), *ISA Transactions*, and *Applied Energy*. He was also a recipient of the Best Young Researcher in the Arab Student Forum Creative among 61 researchers from 16 countries at Alexandria University, Egypt, in 2011. He also received the Excellent Paper Award from IEEE/CSEE JOURNAL OF POWER AND ENERGY SYSTEMS (SCI IF: 3.938; Q1), in 2021 and 2022. He serves as an Editor for a number of prestigious journals, such as IEEE SYSTEMS JOURNAL, *Computers and Electrical Engineering* (CAEE, Elsevier), *IET Journal of Engineering*, and *Smart Cities*. He has also performed more than 800 reviews for highly prestigious journals, including IEEE TRANSACTIONS ON POWER SYSTEMS, IEEE TRANSACTIONS ON SMART GRID, IEEE TRANSACTIONS ON INDUSTRIAL INFORMATICS, IEEE TRANSACTIONS ON INDUSTRIAL ELECTRONICS, *Energy Conversion and Management*, *Applied Energy*, and *International Journal of Electrical Power & Energy Systems*. He was included in the 2018 and 2019 Publons and Web of Science (WoS) list of the top 1% best reviewers and researchers in the field of engineering and cross-fields over the world.

WALID A. OMRAN received the B.Sc. and M.Sc. degrees in electrical engineering from Ain Shams University, Cairo, Egypt, in 1998 and 2005, respectively, and the Ph.D. degree from the Department of Electrical and Computer Engineering, University of Waterloo, Canada, in 2010. He is currently an Associate Professor with the Faculty of Engineering and Materials Science, German University in Cairo. His research interests include the planning and operation of smart grids, integration of renewable energy systems, and energy storage systems.